Smart Agricultural Technology 12 (2025) 101528

Contents lists available at ScienceDirect

Smart Agricultural Technology

journal homepage: www.journals.elsevier.com/smart-agricultural-technology

Evaluation of winter wheat varieties' responses to nitrogen supply supported by 10-band multispectral aerial imaging: reproducibility over crop seasons and sites

Nicolas Vuille-dit-Bille [a,*], Lilia Levy Häner [a], Silvan Strebel [a], Amanda Burton [a], Noémie Schaad [a], Didier Pellet [a], Nathalie Wuyts [a], Simon Treier [a,b], Paola de F. Bongiovani [a,b], Juan Manuel Herrera [a]

[a] Agroscope, Production Technology and Cropping Systems, Route de Duillier 60, 1260 Nyon, Suisse Switzerland
[b] ETH Zurich, Institute of Agricultural Sciences, Group of Plant Nutrition, Lindau, Switzerland

ARTICLE INFO

Keywords:
Nitrogen management
Winter wheat
UAV
10-band multispectral sensor
Red edge
Random forest

ABSTRACT

Nitrogen (N) fertilization trials require resources to investigate the effects of N on yields, N use efficiency, and soil fertility. Multispectral imaging with drones could deliver more affordable and accurate information to optimize N fertilizers. The current literature lacks evidence of the robustness of vegetation indices (VIs) across sites, seasons, and varieties, with studies relying on multispectral sensors that had five bands or less and one red-edge (RE) band centered around 717 or 730 nm. Additional RE bands may allow for the estimation of VIs relevant for N use with higher accuracy and reproducibility. This study examines (i) whether additional RE bands increase the accuracy and consistency of grain and straw yield and N in the biomass, and (ii) whether the relationships between these parameters and VIs change according to crop stage and winter wheat varieties. The study was conducted at two Swiss sites over three seasons, with N fertilizer treatments varying in timing and rate. We found strong relationships ($R^2 > 0.7$) between VIs and N content in biomass, and grain and straw yield. The NDRE with the RE band centered at 740 nm was the most accurate predictor of yield from measurements conducted at heading ($R^2 = 0.92$) and during grain filling ($R^2 = 0.89$), while the MCARI with the RE band centered at 705 nm, measured before heading, was a stronger predictor of total N at anthesis ($R^2 = 0.9$). Therefore, the additional RE bands improved the accuracy of VIs for optimizing the N fertilization of wheat.

Abbreviations

B	Blue band
CSM	Crop surface model
G	Green band
GIS	Geographical information system
GSD	Ground sampling distance
LAI	Leaf area index
MCARI	Modified chlorophyll absorption ratio index
MTVI	Modified triangular vegetation index
N	Nitrogen
NDRE	Normalized difference red-edge index
NDVI	Normalized difference vegetation index
NIR	Near-infrared band
NUE	N use efficiency
p	P-value
PRIF	Principles of fertilization of agricultural crops in Switzerland
R	Red band
R^2	Coefficient of determination
RE	Red-edge band
RF	Random forest
RMSE	Root mean square error
UAV	Unmanned aerial vehicle
VI	Vegetation index

1. Introduction

Food production must double to adequately feed the growing global population, which is projected to reach 9.7 billion by 2050 [1,2]. Nitrogen (N) fertilization is one of the most important agronomic practices

* Corresponding author.
E-mail address: nicolas.vuille-dit-bille@agroscope.admin.ch (N. Vuille-dit-Bille).

https://doi.org/10.1016/j.atech.2025.101528
Received 11 August 2025; Received in revised form 8 October 2025; Accepted 8 October 2025
Available online 15 October 2025

for increasing crop productivity and is a critical input for securing the food of >50 % of the human population [3]. The amount of N fertilizer applied each year has reached 108 million tons [4]. Insufficient N fertilization can lead to a reduction in plant photosynthetic capacity, negatively affecting grain yield and quality [5], while excessive N fertilization has both environmental and economic consequences [6,7]. Excess N is prone to losses through leaching, volatilization, and denitrification, negatively impacting water quality, farming profitability, and increasing greenhouse gas emissions [8]. Adapting N fertilization according to crop needs is an important step toward reducing N losses to the atmosphere or water bodies without affecting crop performance [9].

Winter wheat (*Triticum aestivum* L.) is one of Switzerland's most cultivated field crops [4] and requires optimal quantities of N to produce a high-yielding and high-quality crop with minimal environmental impact [10]. Fertilization directives for Switzerland are described in the "Principles of fertilization of agricultural crops" [11]. As for most countries, the regular updating and improvement of N fertilization directives require dedicated trials, time, and resources. Nitrogen fertilization trials have been widely used to investigate the effects of N fertilizers on crop yields, N use efficiency, and soil fertility, diagnose crop N needs [12,13], and determine the optimal N rates and number of split applications according to development stages to minimize N loss [11,14,15].

Non-destructive sensing methods have been proposed to assess processes that affect N uptake, including crop growth [16,17]. For example, lighter green leaves due to lower N availability can be detected both qualitatively with visual determinations and quantitatively with remote sensing methods [5]. Remote sensing methods, such as unmanned aerial vehicles (UAVs), allow for the achievement of high temporal and spatial resolution, as measurements can be repeated over short time periods and cover larger areas and potentially more variable [18,19]. Vegetation indices (VIs) to detect canopy changes over time have been developed by investigating spectral patterns [20,21] using multispectral and hyperspectral sensors [22]. These investigations mainly focused on the farm level, while the possible applications of these VIs for N fertilization trials remain less explored.

Computing VIs from spectral bands in the near-infrared (NIR) and red-edge (RE) regions of the electromagnetic spectrum showed consistent correlations with parameters that are of interest in N fertilization trials, such as biomass and N content of wheat, maize, and sugar beet [23,24]. The RE spectral band may improve crop N status prediction [25], as was also found in recent research in Switzerland that focused on variable N rate application [26]. In another study, the prediction of biomass N content was not improved by an RE band, but RE showed a more consistent pattern related to N status across vegetative crop growth and a higher reflectance than the red spectral band [27]. A significant correlation was also found between the total N of above-ground biomass and VIs that excluded an RE band obtained with a UAV carrying a multispectral sensor [28]. These contrasting outcomes may be due to confounding stress factors, such as water limitation, as both water stress and N status can change reflectance in the near and middle infrared spectral bands [29]. During the early stem elongation of wheat, RE spectral bands proved to accurately detect N canopy status independently of water limitation and differences in soil cover produced by this stress spectral signal [30,31]. New multispectral sensors that integrate more and narrower RE and NIR bands may allow the delivery of more robust parameters targeted by N fertilization trials.

In this study, we aim to determine: (i) whether the use of three RE bands, rather than one, results in more accurate and consistent estimations of N in the biomass, leaf chlorophyll content, leaf area, and grain yield, and (ii) whether the relationships between these parameters and vegetation indices depend on crop stage and varieties.

2. Materials and methods

2.1. Study area and growing conditions

The field trials are described in detail in Burton et al. [15] as well as in the main agronomical results. Between 2020 and 2022 (harvest years), experiments with winter wheat (*Triticum aestivum* L.) were conducted at two sites in Switzerland: Changins (46.40° N, 6.23° W) and Reckenholz (47.43° N, 8.52° W). The soils at these locations were identified as cambisols/luvisols [32], featuring sand, silt, and clay contents of 37 %, 36 %, and 27 % in Changins and 36 %, 38 %, and 26 % in Reckenholz, respectively. In Changins, the preceding crops were soybean (*Glycine* max) in 2020 and 2021 and sunflower (*Helianthus annuus* L.) in 2022. In Reckenholz, the preceding crop was potato (*Solanum tuberosum* L.) in all years. At both experimental sites, precipitation was higher in 2021 than in the other years, while 2022 was notably drier. Between 2020 and 2022, Reckenholz experienced, on average, higher precipitation (1180 mm) and cooler temperatures (10.0 °C) compared to Changins (1050 mm and 11.0 °C). The N mineralization potential of the soil (0–60 cm), as measured after winter, was comparable at both sites in 2020 and 2021 (Changins: 41.8 and 27.7 kg N ha^{-1}, respectively; Reckenholz: 41.4 and 26.4 kg N ha^{-1}, respectively). In 2022, the mineralization potential was higher in Reckenholz than in Changins (59.0 vs. 28.3 kg N ha^{-1}).

2.2. Field trial design

The experiments included two factors: N fertilizer treatment and winter wheat variety. The experiment in Changins was arranged in a complete randomized block design with two repetitions in 2020 (32 plots), and three repetitions in 2021–2022 (75 plots). In Reckenholz, the experiment used a split-plot design—the N fertilizer as the main treatment and the variety as the sub-treatment—with three repetitions (75 plots). In 2020, plots measured 12 m in length and 12 m in width. Plot dimensions were adjusted in 2021–2022 to increase the number of repetitions, N fertilizer treatments, and varieties. For this, the plot size was reduced to 6 m in length and 3 m in width at Changins. At Reckenholz, the plots were further narrowed to 2 m in width while maintaining a 6 m length.

2.3. Winter wheat varieties

Five high-quality (according to protein content and breadmaking criteria) Swiss varieties of winter wheat were included in the trials: CH_Camedo, CH_Claro, Montalbano, CH_Nara, and Runal (Table 1). Runal was cultivated in the 2021 and 2022 seasons, while the other varieties were grown in all three seasons. At both sites, seeds were sown at 350 viable seeds m^{-2} but row spacing differed slightly, with 0.19 m in Changins and 0.21 m in Reckenholz. The sowing occurred either in October or November, depending on the year's specific weather conditions, while the harvest took place around mid-July, in general [15]. The main agronomic characteristics of the varieties included in the

Table 1
Agronomic characteristics of the five winter wheat varieties grown in the study.

Parameter	CH_Nara	CH_Camedo	CH_Claro	Runal	Montalbano
Height	Very short	Short	Rather short	Moderate	Moderate
Heading	Rather late	Rather late	Rather early	Rather early	Late
Grain protein content	Very high	High	High	Very high	Very high
Grain yield	Moderate	Moderate	Rather high	Moderate	High

Source: Swiss granum [33].

experiments are shown in Table 1.

2.4. Nitrogen fertilization treatments

Six N treatments were applied differently according to the seasons: N0 (0 kg N ha^{-1}), N1 (80 kg N ha^{-1}), N2 (80 kg N ha^{-1}), N3 (160 kg N ha^{-1}), N4 (160 kg N ha^{-1}), and N5 (160 kg N ha^{-1}), as shown in Table 2. The N treatments with the same dose differed in the splitting application strategies.

2.5. Ground-based measurements

Ground-based observations were carried out during the entire growing season to assess the growth and development of winter wheat. At both Changins and Reckenholz, each plot was split into two sections, allowing both manual sampling and harvesting with a combine. In 2020, four areas measuring 7 m in length and 1.5 m in width were harvested within the plot area (12 $m \times 12$ m). In 2021 and 2022, the harvest area of the combine was 1.5 m wide and 4 m long. From booting (BBCH41) until anthesis (BBCH69), chlorophyll content measurements were performed using the device N-Tester® (Yara International ASA, Oslo, Norway) on 30 representative flag leaves per plot. In parallel, on the same plots, leaf area index (LAI) was estimated using a ceptometer (AccuPAR LP-80 Ceptometer, Decagon Devices®, Pullman, Washington state, USA). Three measurements along the row and three others perpendicular to the row were performed to account for the architectural variability of the varieties. For both the N-Tester and LAI measurements, the average results are reported in the comparison with VIs. The total aboveground biomass (kg ha^{-1}) was assessed at flowering and shortly before harvest (data not shown). Two rows of wheat measuring 0.6 m (0.3 m in 2020) were harvested 2 cm above the soil surface. Samples were first weighed while fresh, then dried at 50 °C until a stable weight was achieved, usually taking around 48 h. After drying, they were weighed again to determine their dry mass.

The grain and straw (only in Changins) were harvested after physiological maturity using a combine harvester (Zürn 150, Schöntal-Westernhausen, Germany). The grain from a subsample was then separated from other plant debris (e.g., chaff) to correct the final grain weight. Grain yield is reported on a dry weight basis (0 % moisture). The dried grains and straw were ground to 0.75 mm. The N content of the ground samples was measured using NIR spectroscopy using a ProxiMate (Buchi, Flawil, Switzerland).

Table 2
N treatments applied over the three crop seasons (2020–2022), including three main N treatments (zero, reduced, and conventional) differing in terms of splitting strategies.

N treatment	1st N BBCH 21 kg N ha^{-1}	2nd N BBCH 31	3rd N BBCH 39	Total N	N treatments	Year of harvest
N0	0	0	0	0	Zero	2020; 2021; 2022
N1	20	40	20	80	Reduced	2021; 2022
N2	20	60	0	80	Reduced	2021; 2022
N3	40	80	40	160	Conventional	2020; 2021; 2022
N4	40	120	0	160	Conventional	2020; 2021; 2022
N5	40	40	80	160	Conventional	2020

2.6. Multispectral image acquisition and processing

Multispectral images were acquired using a DJI Inspire 2 drone (DJI, Shenzhen, China) carrying a Micasense RedEdge-MX dual-camera system. The RedEdge-MX dual camera system captures reflectance in 10 spectral bands with wavelengths centered at 444 (bandwidth: 28), 475 (bandwidth: 32), 531 (bandwidth: 14), 560 (bandwidth: 27), 650 (bandwidth: 16), 668 (bandwidth: 14), 705 (bandwidth: 10), 717 (bandwidth: 12), 740 (bandwidth: 18), and 832 nm (bandwidth: 57 nm). It measures incoming sunlight using a downwelling light sensor attached on top of the UAV. This sensor has already been used for studying late-blight potato disease [34]. However, to the best of our knowledge, it has not yet been applied in the context of N fertilization trials. It is important to note that other makers, such as Spectral Devices (Canada), Mapir (United States), and Agrowing (Israel), have made multispectral sensors with multiple RE bands available in recent times. Thus, the outcomes of this study have a wider scope of application than one sensor.

When possible, UAV flights were done before each N fertilization application (BBCH21, BBCH31, and BBCH39) and at key growth stages of winter wheat, namely booting (BBCH41), heading (BBCH59), and anthesis (BBCH65–69). This was especially the case at Changins, while at Reckenholz, UAV survey frequency was lower due to logistic issues (the site was located approximately 250 km away in an area with restrictions on flying UAVs because of an International Airport). As the optimal conditions for multispectral imaging surveys are a clear blue sky with little or no wind, images were taken around solar noon and under sunny conditions, when possible. In total, 31 flights were performed (Table 3). Flight height was set between 30 and 60 m depending on the available batteries and experimental area to cover, resulting in a ground sampling distance (GSD) between 1.85 and 4.08 cm $pixel^{-1}$. Variations in GSD within this range do not generally affect the accuracy of VIs. The overlap in both directions was set to 80 %. Before and after each flight, images of a panel with known reflectance were taken. The images of each flight were mosaicked using the Agisoft Metashape Professional 1.8.4 (Agisoft, St. Petersburg, Russia) structure-from-motion software to create orthomosaics for each UAV flight. The images were radiometrically calibrated before and after each UAV survey using the reflectance panels on the ground and the incident light sensor (only when there was a high variation of light intensity during the flight) on the UAV, with a uniform set of processing parameters used for all flight dates.

2.7. Vegetation index computation

Vegetation indices that consistently showed strong relationships with wheat parameters were identified through sensitivity analysis from a list of 50 candidates (Supplementary Table 1) and examined in detail (Table 4). VIs were computed using the spectral bands from the RedEdge-MX dual-camera system. The selection of a specific RE band from the three available RE bands (centered at 705, 717, and 740 nm) in

Table 3
UAV survey information, including ground sampling distance (GSD) for each crop season (harvest year) and site.

Crop season	Sites	Dates	Flight height (m)	GSD (cm/pix)
2020	Changins	March 11; April 7; May 8, 14, 18, and 28; 3 June	30	1.85
	Reckenholz	April 1; May 25	30	1.89
2021	Changins	March 10; April 1; May 4, 12, 20, and 27; June 3	60	4.08
	Reckenholz	March 23; May 28; June 25	60	4.03
2022	Changins	February 25; March 25; May 4, 10, 18, and 27; June 4	40	2.8
	Reckenholz	March 10; April 6; May 6; June 2 and 15	40	2.77

Table 4
Formula, trait, and reference for the vegetation indices (VIs) reported in the study.

VIs	Formula	Trait	Reference
MCARI*	((RE - R) - 0.2 × (RE - G)) × (RE/R)	N chlorophyll content	[35]
MSR_RE717	((NIR/RE_{717}) - 1)/(((NIR/RE_{717}) + 1)^0.5)	Biomass	[36]
MRENDVI	(RE_{740} - RE_{705})/(RE_{740} + RE_{705} - 2 × *B*)	N chlorophyll content	[37]
MTVI	1.2 × (1.2 × (NIR - G) - 2.5 × (R - G))	Biomass	[5]
MTVI2	(1.5 × (1.2 × (NIR - G) - 2.5 × (R - G)))/((2 × NIR + 1)^2 - (6 × NIR - 5 × (R^0.5)) - 0.5)^0.5	Biomass	[5]
NDRE*	(NIR - RE)/(NIR + RE)	N chlorophyll content	[5]
NDVI	(NIR - R)/(NIR + *R*)	Biomass	[5]
MCARI_MTVI*	MCARI/MTVI	N chlorophyll content; biomass	[5]
MCARI_705_MTVI2*	MCARI_705/MTVI2	N chlorophyll content; biomass	[5]
NDRE_NDVI*	NDRE/NDVI	N chlorophyll content; biomass	[5]

* The red-edge band could be any of three spectral bands in the red-edge region and centered at 705, 717, and 740 nm.

R: red; G: green; RE: red edge; NIR: near-infrared red; MCARI: modified chlorophyll absorption ratio index; MSR: modified simple ratio; MRENDVI: modified red edge normalized difference vegetation index; MTVI: modified triangular vegetation index; NDRE: normalized difference red-edge index; NDVI: normalized difference vegetation index.

the formula is specified when reporting the VIs. For ground measurements at a specific date, such as the total N content in biomass at anthesis, VIs were computed from data with sufficient spectral quality captured at the closest date to the biomass sampling. To predict crop parameters such as total N content in grain, and grain and straw yield at harvest, VIs were computed from a single UAV survey at crop stages ranging from BBCH59 to BBCH69, depending on the availability of UAV surveys. The measured crop parameters were then compared with VIs based on UAV surveys averaged across three key growth stages (pre-heading BBCH41, heading BBCH59, and post-heading BBCH69) for Changins (2020, 2021, and 2022) and Reckenholz (2022). Due to insufficient UAV survey coverage of these crop growth stages at Reckenholz in 2020 and 2021, it was not possible to estimate averages, and single surveys from specific time points were used instead. For time series crop parameters such as N-Tester and LAI, one single UAV survey at crop stage period covering the period of measurements (between BBCH41 and BBCH69) was selected to compute the VIs.

2.8. Data analysis

The orthomosaics were analyzed in the software QGIS (QGIS Development Team 2019, version 3.28). Regions of interest were created for each experimental plot. The spatial extraction of pixel values per VI was done using RStudio Desktop (RStudio Team 2016, version 2023.03.1) with R version 4.2.3 "Shortstop Beagle" [38]. The packages "rgdal," "raster," "stringr," and "data.table" were used. Before computing pixel values, orthomosaics were pre-processed using the R package "FIELDimageR" to exclude soil pixels by means of adaptive threshold segmentation using VIs (single NIR band and NDVI) (https://github.com/filipematias23/FIELDimageR) [39]. This step improved the consistency of the results over the sites and years. Removing soil before computing VIs can be useful to avoid unwanted soil effects and bias, which can lead to misinterpretation of spectral information, especially when soil cover is low in the early stages of winter wheat. The process of image segmentation is commonly used in field crops to improve the reproducibility of VI computations [40]. Visualizations and analysis of the results with scatterplots, boxplots, relationship matrices (from Pearson's correlation), and dendrograms were performed using the R packages "ggplot2," "ggExtra," "gridExtra," "corrplot," "Hmisc," and "openair." The coefficient of determination (R^2) and the root mean squared error (RMSE) parameters from linear and quadratic regressions between VIs and ground-based measurements were estimated using functions available in base R. Clustering analysis was performed using the single linkage method to highlight smaller groups as distinct clusters. Variety differences at each N treatment (zero, reduced, and conventional) were investigated using analysis of variance (ANOVA) and a post-hoc Tukey test to detect significant differences.

A random forest analysis (RF) was conducted on VIs that were consistently related to key wheat parameters, grain yield, straw yield, and total N content in biomass at anthesis (BBCH65). RF is a non-parametric ensemble supervised machine learning algorithm based on decision trees, developed by Breiman [41]. It improves predictive accuracy and controls overfitting by constructing many decision trees during the training process and aggregating their outputs. Each tree is built using a random subset of the data and a random subset of features at each node split, which enhances model robustness and reduces variance in predictions. In this study, RF modeling was used to investigate the differential predictive power of VIs with RE bands centered at 705, 717, and 740 nm to estimate total N content in biomass at anthesis, as well as grain and straw yield. Additionally, RF was employed to determine whether VIs could predict grain and straw yield over the course of the season. The analysis focused on seven critical crop growth stages and management time points: before the second N application (BBCH31), at two nodes (BBCH32), before the third N application (BBCH39), at booting (BBCH45), at heading (BBCH55), at anthesis (BBCH65), and during grain filling (BBCH71). This evaluation was performed exclusively at Changins over three growing seasons (2020–2022), as some of these stages were not included at the Reckenholz site.

RF analyses were implemented using the Jupyter Notebook interface (JupyterLab 4.0.11) in Python 3.12.4. Machine learning modeling was carried out with the scikit-learn library (version 1.6.1) using the RandomForestRegressor, with hyperparameters optimized via grid search and five-fold cross-validation. Model performance was assessed by calculating the coefficient of determination (R^2) and the root mean squared error (RMSE) for both the training and independent test datasets. Feature importance scores were used to identify the most informative spectral–temporal features, reflecting each VI contribution to model predictions. These scores were visualized using matplotlib (3.10.0) and seaborn (0.13.2).

Fig. 1 provides a summary of the data collection materials and processing steps.

3. Results

3.1. Crop N status estimation

The relationship between three main crops N components, total N in biomass at anthesis, the chlorophyll content (measured by a chlorophyll meter, N-Tester), the N in the grain at harvest, and spectral information (single bands, single VIs, and combined VIs) obtained using a UAV-mounted sensor was examined by means of linear regression (Fig. 2; Supplementary Table 2). Total N in biomass at anthesis showed consistent relationships with UAV spectral information. The coefficient of determination (R^2) between total N in biomass and the combined VI NDRE705_NDVI was greatest in Changins 2020 ($R^2 = 0.92$). This combined VI was also the most accurate predictor of total N in biomass in 2021 ($R^2 = 0.74$) and 2022 ($R^2 = 0.63$) in Changins. In Reckenholz, the relationships between total N in biomass at anthesis and spectral information were, overall, weaker compared to Changins

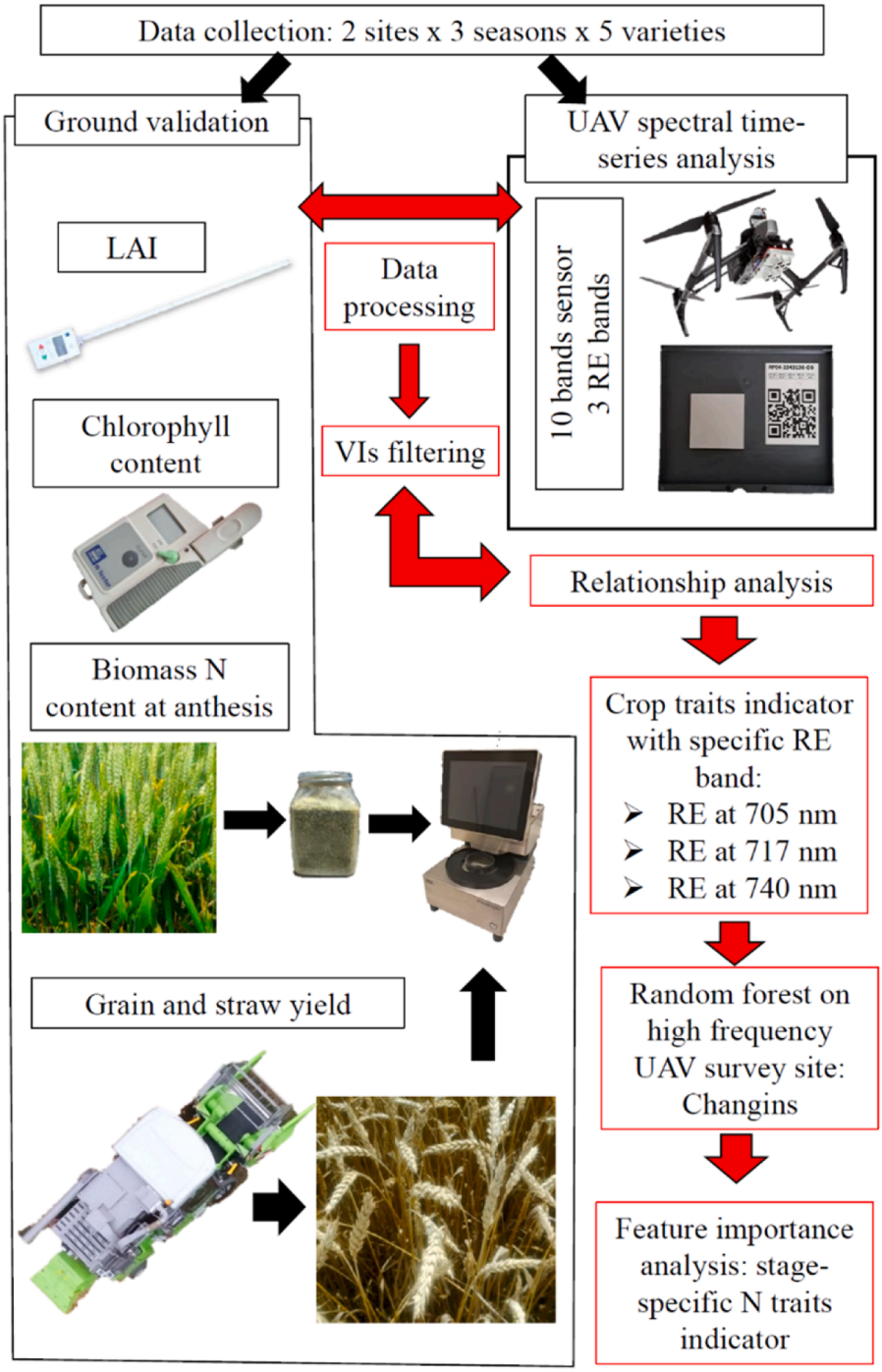

Fig. 1. Overview of the data collection and processing workflow.

(NDRE705_NDVI: R^2 = 0.47, 0.60, and 0.23 for 2020, 2021, and 2022, respectively).

The regression between NDRE705_NDVI and total N in biomass was a better fit using a quadratic than a linear regression in one case (Changins 2021), but overall, the R^2 did not significantly change (Fig. 3). The scatter plots grouped by year and site showed different patterns according to site (Fig. 3). In 2020 and 2021 in Changins, there were contrasted levels of total N in biomass at anthesis in line with the three main N treatments (zero, reduced, and conventional). In the same years, the total N in biomass did not form clusters according to the main N treatments in Reckenholz. In 2022, the difference between the N treatments was comparable in Changins and Reckenholz.

Three VIs including RE band centered at 705 nm—NDRE705_NDVI, MRENDVI and MCARI_705_MTVI2—showed strong relationships with chlorophyll content in leaves measured using N-Tester. The strongest relationship was obtained in 2022 for NDRE705_NDVI (R^2 = 0.8) in Changins. The MRENDVI (R^2 =0.56–0.73) and MCARI_705_MTVI2 (R^2 =0.65–0.7) showed a consistently strong relationship in Changins over the three years (2020–2022), albeit lower than the NDRE705_NDVI combination. Additionally, MCARI_705_MTVI2 was better at predicting chlorophyll content across seasons in Reckenholz, even though the R^2 values were generally weaker compared to Changins.

The relationships between total N in grain at harvest and VIs were more variable and ranged from strong in 2020 for both sites (R^2 = 0.76 in Changins and R^2 = 0.73 in Reckenholz) to very weak R^2 in 2022 in Reckenholz (R^2 = 0.15). VI-based predictions were less consistent than

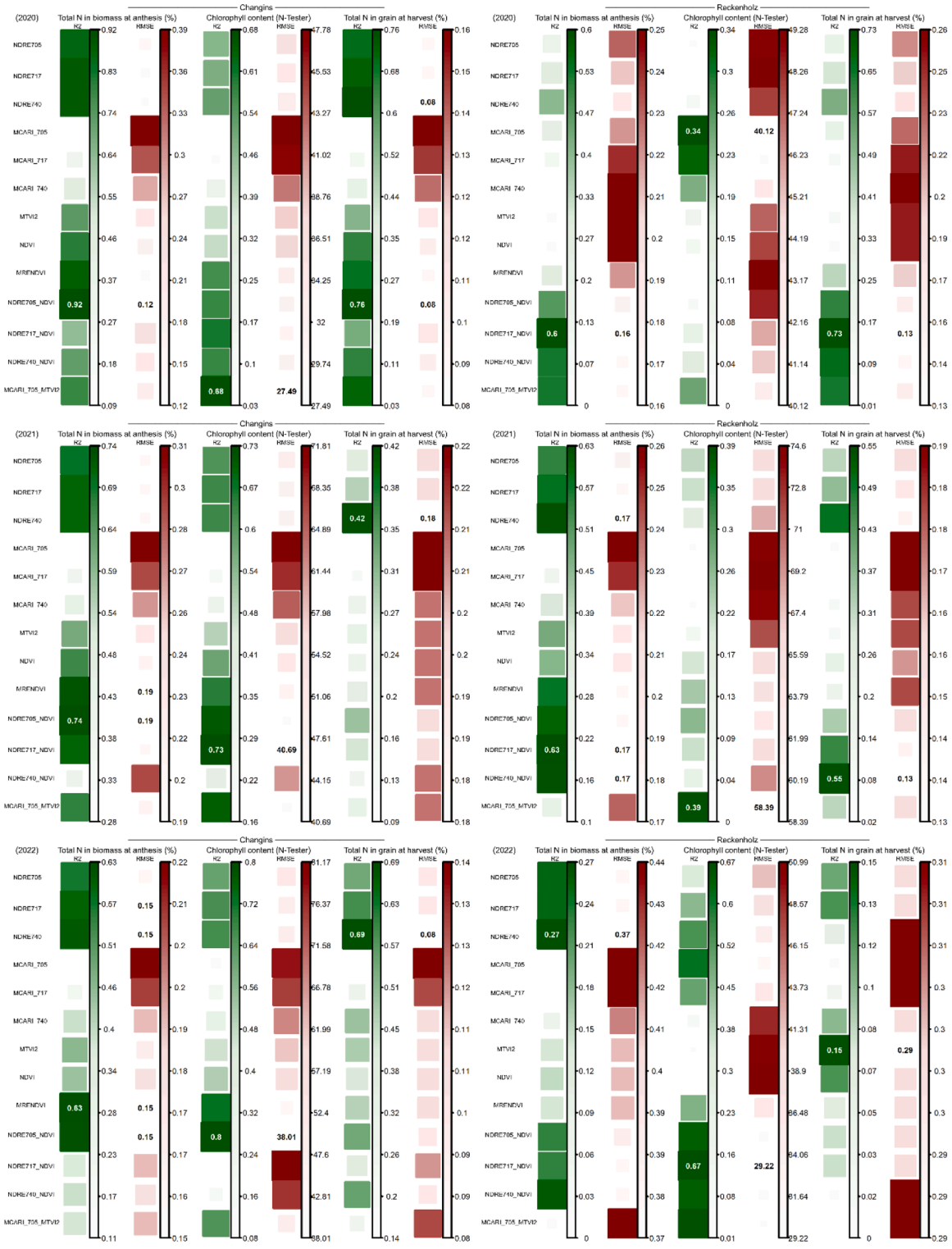

Fig. 2. Relationship matrix between traits linked to wheat N status and vegetation indices (VIs) obtained using a UAV-based multispectral sensor in the crop seasons 2020, 2021, and 2022. The highest coefficient of determination (R^2) and the lowest root mean squared error (RMSE) for each wheat trait are reported across years and sites. Model performance was evaluated using linear regressions, where wheat traits served as dependent variables and single or combined vegetation indices as predictors. The total N in biomass at anthesis (BBCH65) and the chlorophyll content (average of measurements at BBCH45 and BBCH65) are compared to UAV survey dates in the same crop stage period. Chlorophyll content was measured with a N-Tester® (Yara International ASA, Oslo, Norway)**.** Total N in grain is related to UAV survey dates between BBCH59 and BBCH69. R^2 values are shaded from white (low) to green (high), and RMSE values from white (low) to red (high). Square sizes vary from small (low values) to large (high values) based on R^2 and RMSE, enhancing the contrast in the visualization.

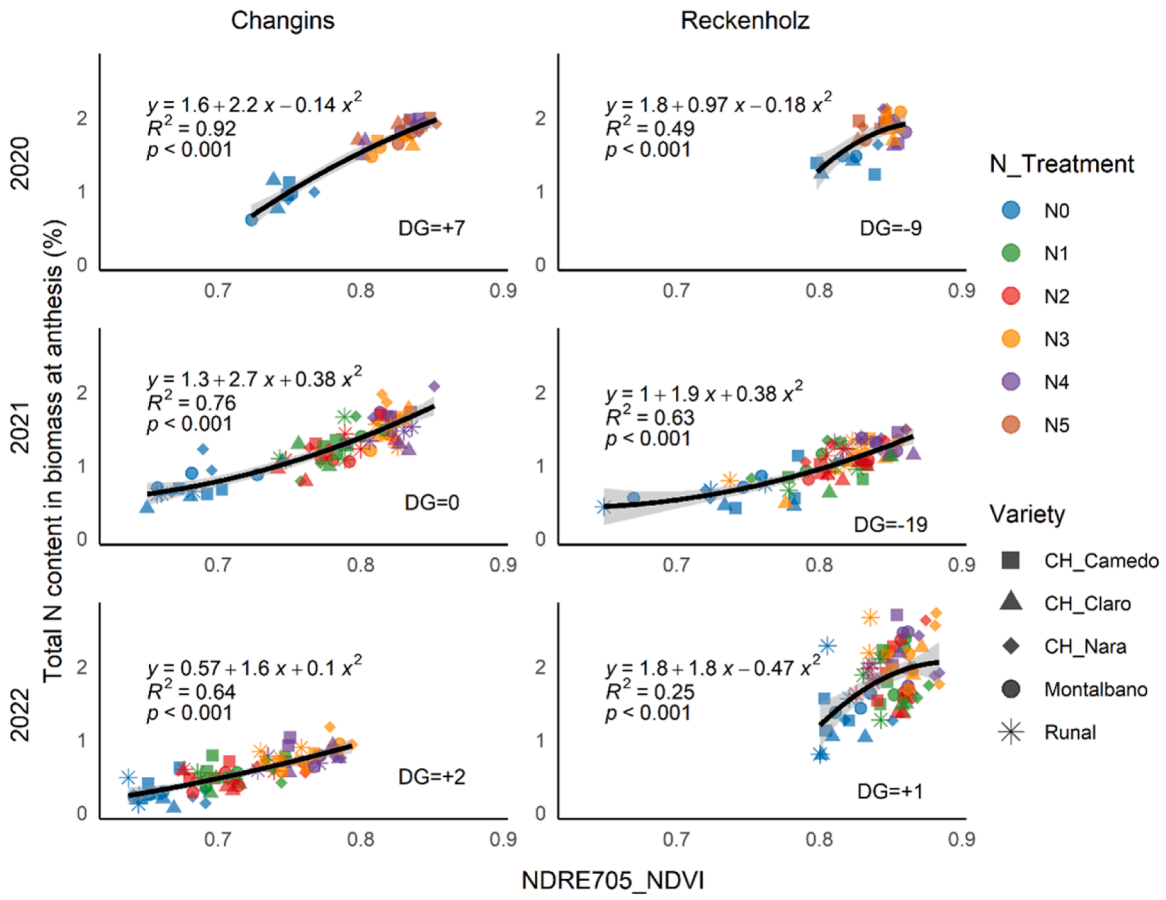

Fig. 3. Relationship between the combined VI NDRE705_NDVI (x-axis) and the total N content in biomass at anthesis (y-axis). Data points are grouped according to varieties (shapes) and N treatments (colors). The total N in biomass at anthesis (BBCH65) corresponds approximately to a UAV survey date at the same crop stage. DG: day gap or number of days between the UAV survey and biomass sampling. The coefficient of determination (R^2), p-value (*p*), and regression equation are shown in the figure for each location (Changins and Reckenholz) and each season (2020, 2021, and 2022). N0 (0 kg N ha^{-1}), N1 (80 kg N ha^{-1}), N2 (80 kg N ha^{-1}), N3 (40–80–40 kg N ha^{-1}), N4 (40–120–0 kg N ha^{-1}) and N5 (40–40–80 kg N ha^{-1}).

the total N in biomass at anthesis and chlorophyll content in leaves. The NDRE705_NDVI was again one of the best-performing VIs at predicting total N content in grain at harvest, with the strongest relationship in 2020 in Changins ($R^2 = 0.76$).

3.2. *Prediction of crop yield, biomass, and leaf area*

Fig. 4 shows the relationships between grain yield and VIs (based on a single UAV survey in the crop stage period ranging from BBCH59 to BBCH69. NDRE740 had the strongest relationship with grain yield in 2021 for Changins ($R^2 = 0.93$). NDRE717 and NDRE705 performed better than NDRE740 in predicting grain yield at Reckenholz in 2021 and at Changins in 2021 and 2022, and had a consistent and strong relationship with grain yield. The R^2 varied between 0.59 and 0.92 and was comparable to the NDRE740 predictions, considering all years and sites. As grain yield is a complex trait that may not be estimable by a single UAV survey, flights from several crop stages (BBCH41, BBCH59, and BBCH69) were considered, and the average VI values were computed for Changins and Reckenholz in 2022 (Fig. 5). The average NDRE717 across the three UAV surveys slightly improved the R^2 (Fig. 6). As observed in the analysis of total N in biomass, grain yield was also impacted by the site and season.

Straw yield was only measured in Changins and showed consistent relationships with several VIs (Fig. 4). The strongest relationship was obtained when comparing straw yield and a single blue band (444 nm, $R^2 = 0.87$; Supplementary Table 3). Furthermore, four VIs—NDVI, NDRE705, MCARI_740, and MCARI_740_MTVI—had high R^2 values, varying from 0.72 to 0.84 across seasons. The MCARI_740_MTVI was further examined using scatterplots (Fig. 7). The relationships improved for each crop season when considering the average spectral values of several UAV surveys during critical growth periods of wheat (BBCH41, BBCH59, and BBCH65), as well as using quadratic regression. Discrimination of points within the N treatment blocks (0 kg N ha^{-1}, 80 kg N ha^{-1} and 160 kg N ha^{-1}) and varieties was also clearly visible in the scatter plots with high values, with high straw biomass for CH_Claro, Montalbano, and Runal compared to low values for CH_Nara and CH_Camedo (Fig. 7). Overall, a strong relationship was found between straw yield and VIs when combined with the RE band centered at 740 nm; however, these VIs did not show any relevant relationship with grain yield (Fig. 4).

For the leaf area index measured with a ceptometer, contradictory results were obtained. Overall, the link between the RE band centered at 740 nm and wheat biomass was not confirmed because VIs containing other RE bands performed better for LAI prediction (e.g., NDRE705 and NDRE717 compared to NDRE740). In general, single rather than combined VIs had better relationships with LAI (Fig. 4).

3.3. *Consistency and reproducibility of VIs for different wheat traits*

Fig. 8A shows the relationship between the studied wheat parameters and the most promising VIs for Changins and Reckenholz across the three crop seasons (2020, 2021, and 2022). The analysis highlights the relationships between VIs based on different RE bands and the key traits of wheat (Fig. 8A). The VIs computed with the RE band centered at 705

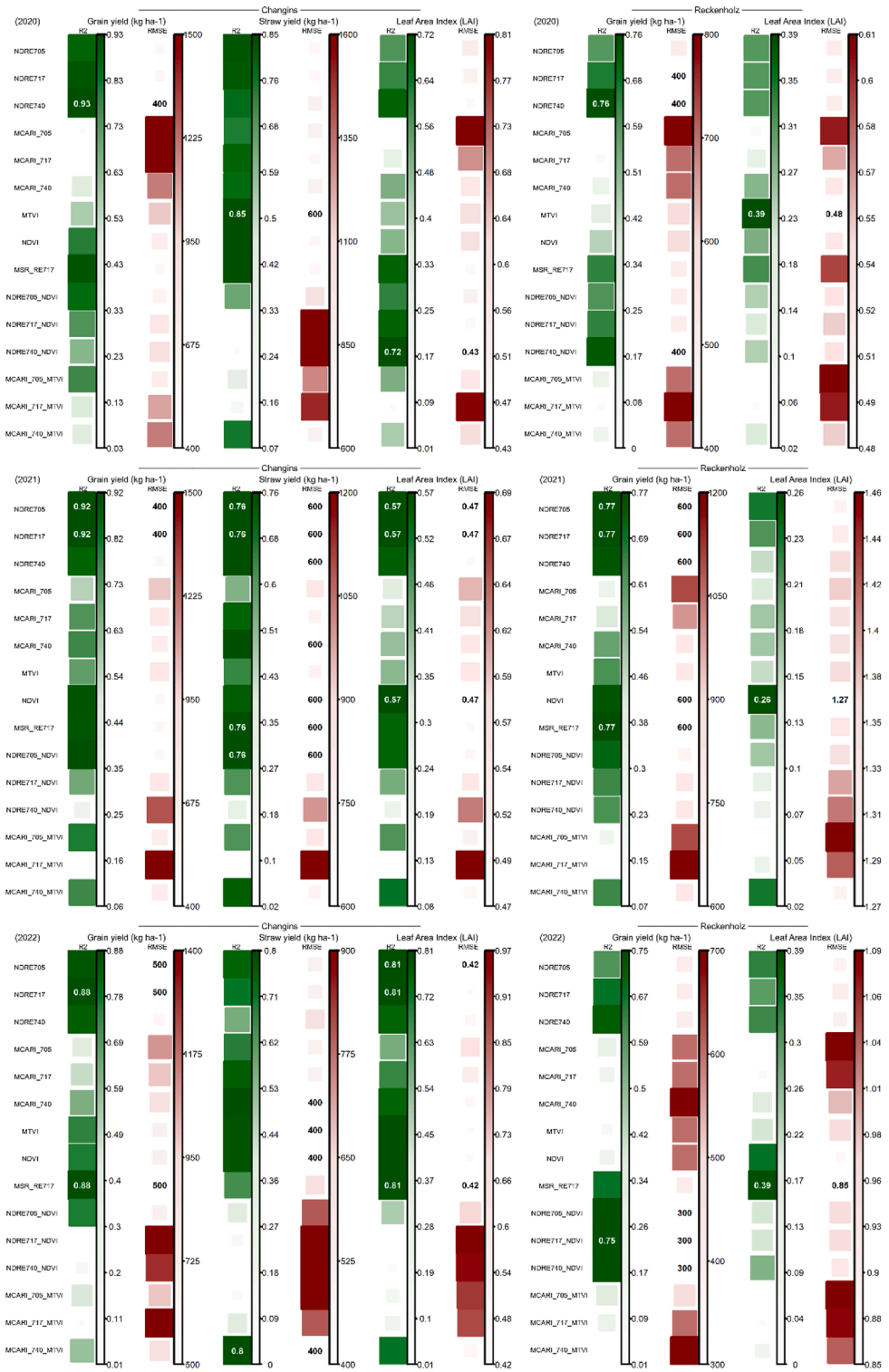

Fig. 4. Relationship matrix between wheat traits related to yield components and vegetation indices (VIs) obtained using a UAV-based multispectral sensor in the crop seasons 2020, 2021, and 2022. The highest coefficient of determination (R^2) and the lowest root mean squared error (RMSE) for each wheat trait are reported across years and sites. Model performance was evaluated using linear regressions, where wheat traits served as dependent variables and single or combined vegetation indices as predictors. Grain and straw yield were related to spectral data from a UAV survey date between BBCH59 and BBCH69, depending on the available data. The LAI (average of measurements at the BBCH45 and BBCH65 stages) was compared with a UAV survey date in the same crop stage period. R^2 values are shaded from white (low) to green (high), and RMSE values from white (low) to red (high). Square sizes vary from small (low values) to large (high values) based on R^2 and RMSE, enhancing the contrast in the visualization.

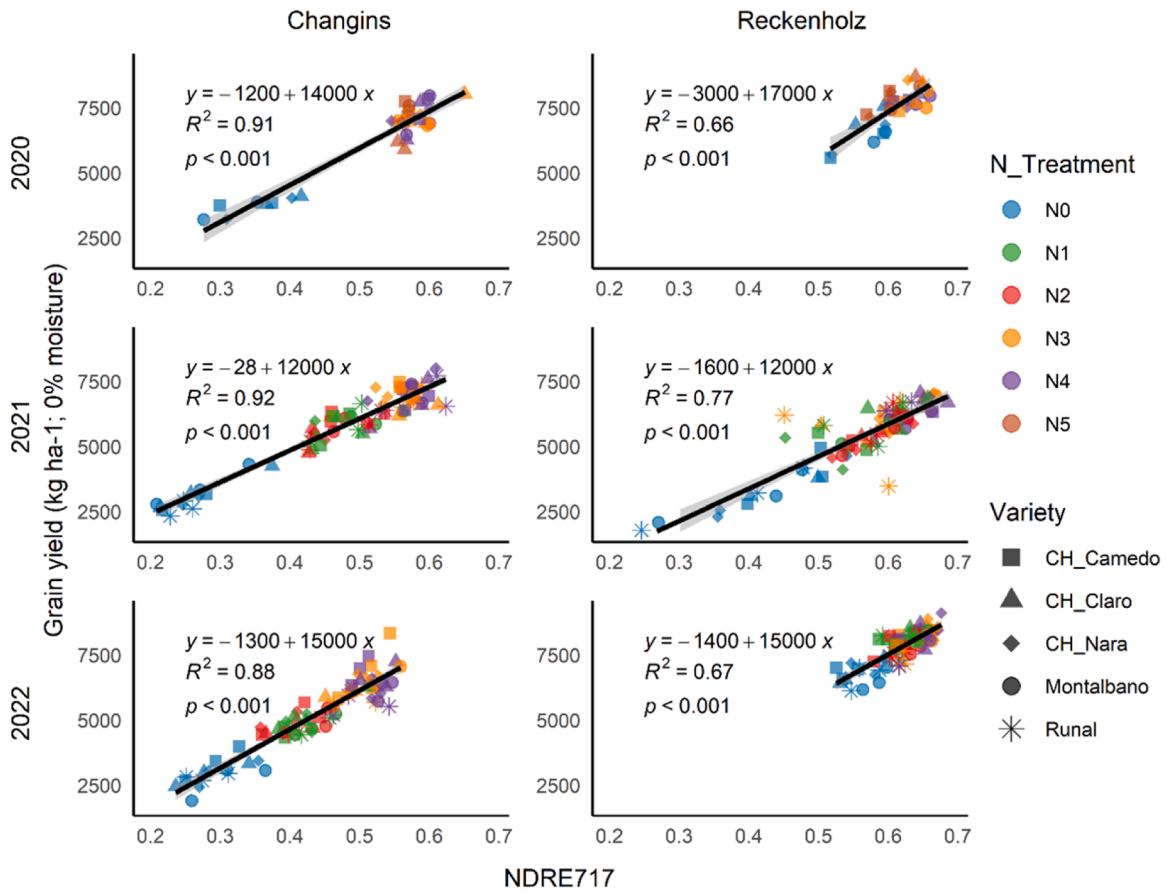

Fig. 5. Relationship between NDRE717 (x-axis) and grain yield at harvest (y-axis). Data points are grouped according to varieties (shape) and N treatment (color). NDRE717 was averaged across three UAV surveys linked to key crop stages (BBCH41, BBCH59, and BBCH65). In 2020 and 2021 for Reckenholz, only one single UAV survey between BBCH59 and BBCH65 was used due to the lower flight frequency. The coefficient of determination (R^2), p-value (p), and regression equation are shown in the figure for each location (Changins and Reckenholz) and each season (2020, 2021, and 2022). N0 (0 kg N ha^{-1}), N1 (80 kg N ha^{-1}), N2 (80 kg N ha^{-1}), N3 (40–80–40 kg N ha^{-1}), N4 (40–120–0 kg N ha^{-1}) and N5 (40–40–80 kg N ha^{-1}).

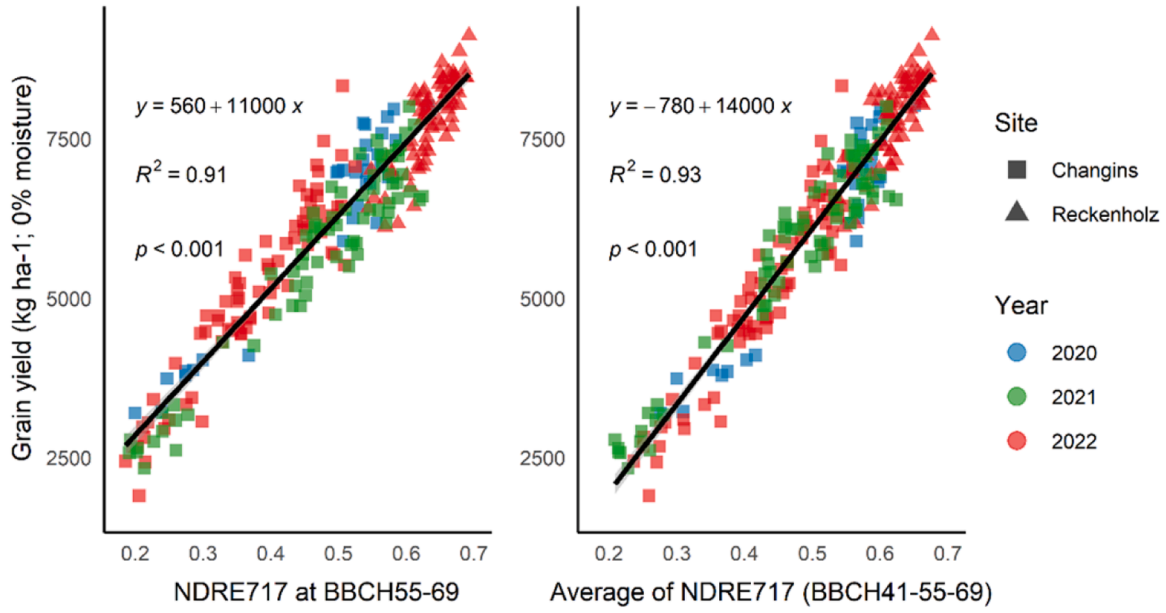

Fig. 6. Relationship between NDRE717 (x-axis) and grain yield at harvest (y-axis) based on a single survey date (left) and multiple dates (right). Data points are grouped according to site (shape) and season (color). NDRE717 based on a single UAV survey between BBCH59 and BBCH69 (left) is compared to the average of NDRE717 on three UAV survey dates (right). Reckenholz 2020 and 2021 are excluded because there were not enough UAV surveys to calculate the average for the same crop growth period. The coefficient of determination (R^2), p-value (p), and regression equation are shown in both scatter plots.

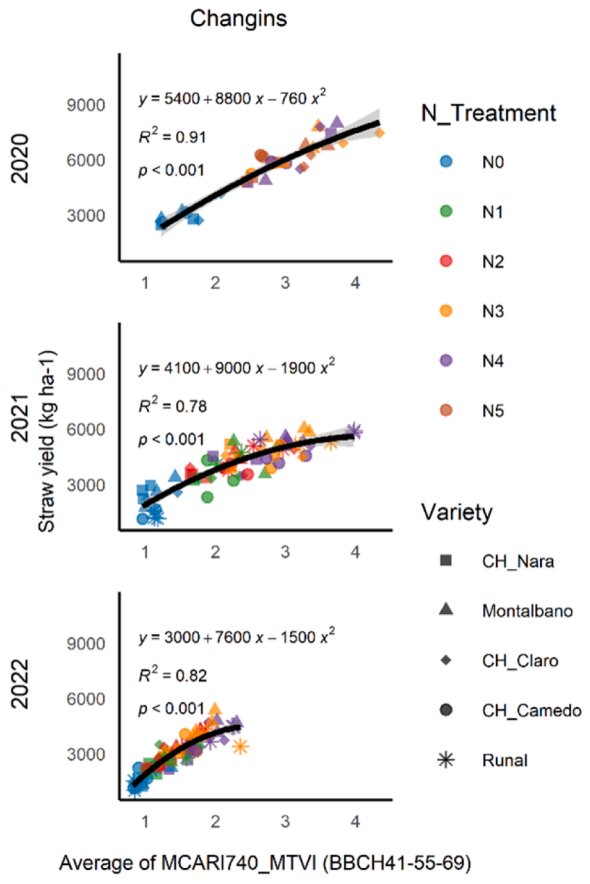

Fig. 7. Relationship between the combined MCARI_740_MTVI (x-axis) and straw yield at harvest (y-axis). Data points are grouped according to varieties (shape) and N treatment (color). MCARI_740_MTVI was averaged across three UAV surveys linked to key crop stages (BBCH41, BBCH59, and BBCH65). The coefficient of determination (R^2), p-value (p), and regression equations are shown for Changins during three crop seasons (2020, 2021, and 2022) and five N treatments (N0: 0 kg N ha^{-1}, N1: 80 kg N ha^{-1}, N2: 80 kg N ha^{-1}, N3: 40–80–40 kg N ha^{-1}, N4: 40–120–0 kg N ha^{-1}, and N5: 40–40–80 kg N ha^{-1}).

nm—NDRE705_NDVI, MRENDVI and MCARI_705_MTVI2—were the most consistent predictors of N content in biomass at anthesis and chlorophyll content in leaves across sites and years. For grain N content at harvest, relationships were generally weaker compared to the other relationships between VIs and crop traits, and no clear discrimination was observed between VIs using the RE band centered at 705 nm and those using the other RE bands. Notably, NDRE705_NDVI also presented a strong relationship with other crop traits, such as grain ($R^2 = 0.73$) and straw yield ($R^2 = 0.66$). Grain yield achieved the strongest relationship with VIs using RE bands centered at 717 nm, such as NDRE717 (N chlorophyll content indicator) and MSR_Rede717 (biomass indicator). Finally, the VI combined with the RE band centered at 740 nm (MCARI_740_MTVI) did not show consistent relationships with the main crop traits, except for straw yield, for which the relationship was strong ($R^2 > 0.83$) and consistent across both sites and years.

The dendrogram in Fig. 8B provides additional information concerning the relationships between all variables. MCARI_705_MTVI2 seemed different compared to other VIs and was classified in a separate cluster. The total N content in grain at harvest and chlorophyll content were closely related to the total N at anthesis. The grain yield was grouped with VIs, including the RE band centered at 717 nm (NDRE717 and MSR_Rede717) and at 705 nm (NDRE705_NDVI and MRENDVI). Straw yield and VI MCARI_740_MTVI, which showed the strongest R^2 in the relationship matrix, were in the same cluster and closely related to LAI and total N at the anthesis.

The random forest model achieved the highest predictive performance for grain yield ($R^2 = 0.92$ and RMSE = 410 kg N ha^{-1}). Similarly, strong results were obtained for straw yield (train $R^2 = 0.89$ and RMSE = 464 kg N ha^{-1}) and total N in biomass (train $R^2 = 0.9$ and RMSE = 0.2 %). For both grain and straw yield prediction, NDRE centered at 740 nm emerged as the most important predictor, though at different crop stages: at heading for grain yield and during grain filling for straw yield (Fig. 9A and 9B). By contrast, the prediction of total N content in biomass at anthesis was most strongly influenced by the MCARI VI centered at 705 nm, measured during stem elongation and before the third N application (Fig. 9C).

3.4. Winter wheat varieties

The performance of individual varieties for three main wheat traits (total N in biomass at anthesis, and grain and straw yield) was compared

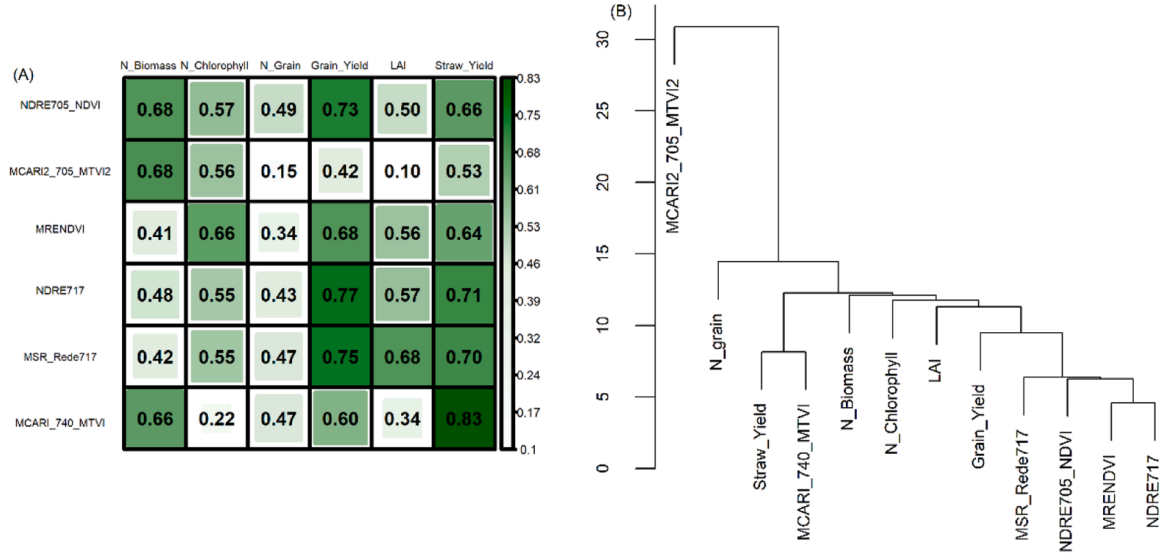

Fig. 8. Relationship matrix (A) and dendrogram (B) including the most promising VIs and crop traits. The coefficient of determination (R^2) values are reported in the relationship matrix. The components (traits or VIs) linked to nitrogen, grain yield, and biomass are highlighted with colors from white to green for low and high R^2 values, respectively. The dendrogram height indicates the degree of dissimilarity between the clusters.

Fig. 9. Ten most important vegetation indices VIs identified by random forest analysis for predicting (A) grain yield, (B) straw yield, and (C) total N content in biomass at anthesis (BBCH65) in Changins across three growing seasons (2020–2022). Time-specific VIs are labeled by crop growth stages.

with the values obtained for VIs by means of analysis of variance and boxplots (Fig. 10) for conventional N treatment levels (N3, N4, and N5). The analysis was further extended for the reduced (N1 and N2) and zero (N0) N treatment levels (Supplementary Figs. 2 and 3). CH_Nara showed higher overall values compared to the other varieties for both N content in biomass at anthesis and NDRE705_NDVI across years and sites. There were some exceptions for Reckenholz in 2020 and 2021, where the VI patterns did not follow the same trend observed for the wheat parameters, with lower values compared to other varieties, such as Montalbano.

Montalbano generally produced the highest grain yield. This observation was confirmed with NDRE717, which aligned well with the VI values. However, in 2022 at Changins, Montalbano was less productive than most of the other varieties, yet the NDRE717 predictions indicated high values for this variety, suggesting a discrepancy. At Reckenholz, another variety, CH_Claro, also had high grain yield and high values for NDRE717 over the three years (2020–2022). In 2022 in Reckenholz, Runal had a particularly low grain yield, and this observation was also

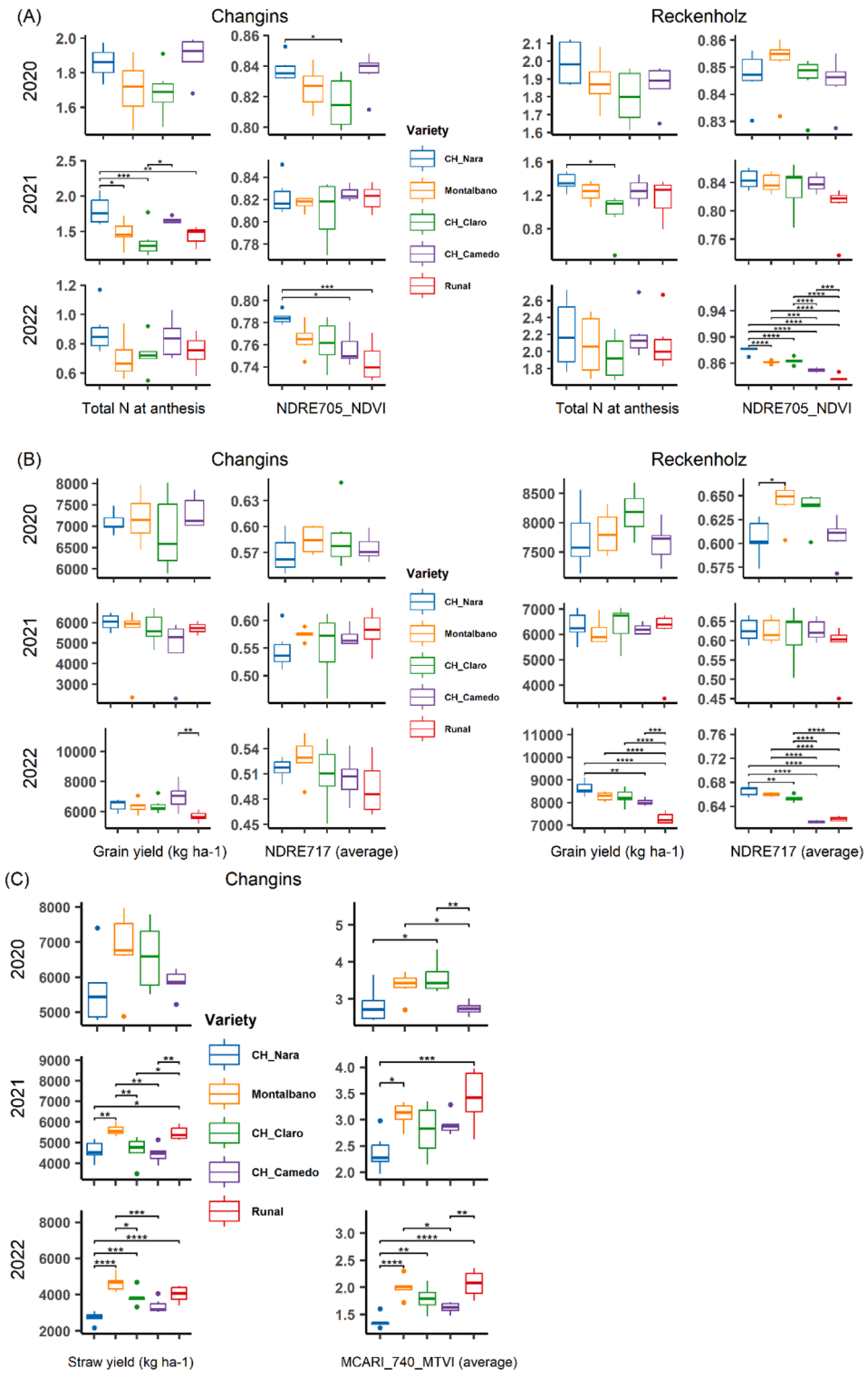

Fig. 10. Comparison between crop traits and VIs for conventional N treatments (average of N3, N4, and N5) across crop seasons (2020, 2021, and 2022). For each of the following components, vegetation indices, N in biomass at anthesis (A), grain (B), and straw (C) yield at harvest, an analysis of variance between varieties was performed, and results of a post-hoc Tukey test are shown by means of significance levels: * = $p < 0.05$, ** = $p < 0.01$, *** = $p < 0.0001$. MCARI_740_MTVI and NDRE717 were averaged across three UAV surveys linked to key crop stages (BBCH41, BBCH59, and BBCH65) to be compared to dynamic crop traits, such as grain and straw yield.

noticed with low values of NDRE717.

The straw yield at harvest was measured only in Changins. For this parameter, the variations were mainly explained by varieties and were consistent over the years and sites, which is in line with MCARI_740_MTVI. Montalbano, CH_Claro, and Runal showed high straw yields in Changins over the three years (2020–2022) compared to CHNara and CH_Camedo. In addition, the MCARI_740_MTVI delivered different information compared to NDRE705_NDVI and NDRE717 and was strongly correlated to the straw yield parameter, with the same difference trends between varieties. For example, in Changins in 2022,

CH_Nara had high values for total N in biomass at anthesis (NDRE705_NDVI) and grain yield (NDRE717), but a low value for straw yield (MCARI_740_MTVI).

4. Discussion

4.1. Potentialities of 10-band multispectral aerial imaging for N fertilization trials

The results of this study show that a 10-band multispectral aerial sensor allowed the prediction of N ($0.27<R^2<0.92$) and chlorophyll ($0.36<R^2<0.80$) content in the biomass of winter wheat from UAV surveys conducted before grain filling (Fig. 2). Biomass and its N content are central parameters targeted by N fertilization trials because they allow estimation of the N Nutrition Index (NNI), which is a reliable indicator of wheat N status. However, its determination is laborious and expensive when it depends on the conventional practice of taking destructive biomass samples [42]. In this study, we reliably assessed biomass N content over crop seasons, N treatments, and sites in less time and with fewer resources using a UAV. Since critical N concentration levels for the NNI should be estimated practically for the entire vegetative period of wheat, UAV multispectral imagery can improve the information that N fertilization trials deliver to farmers. Although predictions of grain yield and grain N content before harvest, straw yield, and LAI have not generally been of central interest in N fertilization trials, they could make N fertilization trials more informative and increase their range of application. Here, our method predicted grain yield from multispectral images collected before the onset of grain filling with a R^2 that ranged from 0.76 to 0.93wiwww, while the corresponding values for total N in grain were 0.15 and 0.76. For LAI, the minimum and maximum R^2 values were 0.26 and 0.81, respectively. The predictions of grain N content were generally more accurate from UAV surveys after anthesis (Fig. 2) than from surveys close to physiological maturity (data not shown). Combining UAV estimates of LAI, grain N content, and yield from N fertilization trials with crop growth models [43,44] may allow predictions for in-season modulation and optimization of N fertilizer rates. This can help farmers make more informed decisions about N fertilization during the growing season.

As the importance and awareness of agricultural sustainability grows, the goals of improving crop production and environmental quality converge. Accordingly, N use efficiency (NUE) is an established metric used to benchmark N management from N fertilization trials. Increasing NUE in agriculture remains a main concern in Switzerland, as NUE is low (30 % in 2014) [45] compared to other countries, such as Denmark (41 % in 2012) [46]. There are numerous approaches to calculating NUE that depend on the objective of the calculation, including fertilizer, crop, soil, production system, and landscape perspective [47]. Two parameters, grain yield and N content, that were reliably predicted in this study (Tables 5 and 6) with UAVs are useful for all NUE indicators, particularly for several fertilizer-based indicators (e.g., partial factor productivity, N surplus, and fraction of N allocated to yield N) and crop-based indicators (e.g., N utilization efficiency, internal efficiency, and N harvest index) of NUE. This is particularly useful for characterizing the response of N management on yield, quality, and NUE of winter wheat varieties, as differences among them with implications for N management have been reported [48,49]. For faster improvement in NUE on farms, Sylvester-Bradley et al. [48] suggested conducting breeding and variety testing at some sites with more than one level of applied N and that grain N %, N harvest index, and canopy N ratio (kg N ha^{-1} green area) should be measured more widely. More cost-effective measurements of these parameters with multispectral aerial imaging instead of classic destructive samplings could free resources to increase the number of varieties and levels of applied N. The possibility of accurately estimating biomass N content at anthesis from multispectral aerial imaging, along with N content at harvest, allows the estimation of post-anthesis N uptake of large panels of varieties. Post-anthesis N uptake has been reported as a key trait to improve NUE in winter wheat [50]. These indicators will be useful in the near future when sustainability aspects become mandatory for the registration of varieties in Europe, as expected with a recent update in the legislation on the production and marketing of plant reproductive material [47,51]. Furthermore, variety-specific predictions of biomass, biomass N content, grain yield, and grain N content could lead to a more accurate determination of N needs in specific environments.

In this study, multispectral aerial imaging allowed the prediction of straw yield (Fig. 4), a parameter that is not usually reported in N fertilization trials. This indicates that including straw yield estimates from multispectral aerial imaging in reports of N fertilization trials could provide useful information about the implications of the choice of varieties and N fertilization rates on soil fertility beyond a single growing season. Straw yield estimates can be indicative of the amount of residues left after the harvest and, therefore, the capacity to regenerate soil attributes, such as soil organic matter. Residue management affects soil properties, soil erosion, and crop production [52]. Multispectral aerial imaging can support the determination of threshold levels of straw removal according to soil types, aiming at maintaining or enhancing soil productivity, sustainability, and environmental quality. Therefore, quantifying straw production can provide insights to better manage trade-offs among obtaining extra farm income from selling straw, maintaining soil health by increasing the soil organic matter content, and avoiding high levels of residue that may hinder post-harvest operations, such as planting the succeeding crop [53]. Straw yield along grain yield and above-ground biomass [54,55] can deliver framers a more integrative perspective to make N management decisions.

4.2. Spectral response of winter wheat varieties as related to N status

To the best of our knowledge, previous studies evaluating the responses of winter wheat to nitrogen supply with a multispectral sensor have used only one RE band centered at 717 or 730 nm [26,56] to assess wheat traits related to N status. The VIs that included the RE band centered at 705 nm were strongly correlated with the ground truth measurements for chlorophyll content and total N in biomass at anthesis. This was highly consistent for Changins across the three crop seasons for the combined VI NDRE705_NDVI. Although in Reckenholz, the relationships were weaker compared to Changins, NDRE705_NDVI explained a significant proportion of the variance in two out of three years (Fig. 3). Two main hypotheses are put forward to explain the lower prediction performance in Reckenholz.

First, Reckenholz is a remote experimental site, which led to logistical issues that limited the frequency of flights during the growing season. The VIs for Changins were estimated from several flights, while for Reckenholz, this was generally done from one flight. This shows the accuracy advantage of estimating VIs from more than one flight. In addition, spectral quality is optimized (around noon and without clouds), which could have also led to lower prediction accuracy in Reckenholz, since the requirements to optimize spectral quality could not always be fulfilled (Supplementary Fig. 1). The quality of the ground truth samples may also have introduced some bias. In most years, biomass sampling at anthesis could not be done on the same day as the UAV survey. By contrast, in Changins, the biomass sampling almost perfectly matched the UAV survey dates, and the biomass samples from Reckenholz could not be dried right after they were collected and were usually dried around five hours after collection due to the distance between the field and the drying facilities. This may have led to the degradation of samples due to warm temperatures and humidity [57].

Second, the soil N availability was generally greater in Reckenholz than in Changins; thus, there were fewer contrasted responses to the N treatments than at Changins. Although the N rate was estimated considering soil N content after winter, a higher N mineralization in spring and summer can be expected in Reckenholz compared to Changins. At Changins, the values were uniformly distributed along the VI

values for the three main N treatments (zero, reduced, and conventional supply of N fertilizer), thereby showing stronger relationships between spectral and ground truth data. Reckenholz generally presented greater relative humidity conditions over the season and years compared to the Changins. This may have disturbed the spectral signal, especially in the NIR region, which is sensitive to water content in plant tissues, and variations in moisture content among varieties can affect the plant N content estimation [58].

The plant canopy has high reflectance in the NIR bands, and it is absorptive in the red bands, providing meaningful information about crop growth [54] and plant N levels [59,60]. However, it becomes less reliable at both low and high N levels, which saturates the signal [61, 62]. Therefore, due to the strong relationship between N and biomass [63,64], the most accurate VI for predicting total N in biomass at anthesis was a combination of VIs (NDVI and NDRE705). The combined VI NDVI_NDRE705 also demonstrated adequate sensitivity to detect differences at the variety level (Fig. 10). Specifically, CH_Nara exhibited higher average values for N content in biomass at anthesis, as well as for the combined VI NDRE705_NDVI. This finding is consistent with previous studies that have reported a superior grain N content of this variety compared to others [65,66]. Additionally, the combined VI NDRE705_NDVI effectively predicted total N content in biomass because it isolates foliar pigment signals (closely linked to N) by canceling out shared sensitivities to LAI and soil background present in both NDRE and NDVI [67].

In addition to red (671 nm) and NIR (780 nm) spectral bands, the red edge bands centered at 705 nm showed promising potential to predict N content in biomass and chlorophyll. This is in line with Stone et al.'s [59] and Zhao et al.'s [60] notions that the spectral region from 550 nm to 710 nm is particularly suitable to characterize crop N status. MTCI (MERIS Terrestrial Chlorophyll Index) covering chlorophyll absorption characteristics in the red edge region (around 709 nm) has been linked to chlorophyll content in plants. It also combines reflectance information at 754 nm and 681 nm to reduce soil background noise [58,68]. MRENDVI and MCARI_MTVI2 showed a consistent potential to predict N content in leaves when combined with the red edge band centered at 705 nm (MCARI_705_MTVI2). This VI was quite sensitive, and there was a need to segment images to remove soil background effects, especially at an early stage when the soil was not fully covered. The VI combined with broadbands and RE bands centered between 710 and 735 nm was previously shown to be related with N concentration [18,26], but the relationship was not particularly strong in this study ($R^2 < 0.5$). This VI is described as having the advantage of discriminating small differences between varieties, but here, they performed worse than NDRE705_NDVI. Although portable and non-destructive instruments such as the SPAD-502 Plus (Konica Minolta Optics, Japan) or the N-Tester® (Yara International ASA, Oslo, Norway) are considered more accurate than VIs for measuring leaves with a high chlorophyll content [69], the VIs MRENDVI, MCARI_705_MTVI2 and NDRE705_NDVI were closely related to chlorophyll content measured by a chlorophyll meter. Moreover, VIs from UAV sensors demonstrated more representative measurements, given their coverage of the entire plot.

Predicting total N in grain at harvest, a proxy of grain protein and grain quality, proved to be challenging. We attribute this to the changes that occur in the crops during grain filling. During this period, there is a constant loss of relevant spectral information toward zero until the crop is dry and reaches physiological maturity [70,71]. NDRE integrating the RE band centered at 740 nm showed promising relationships with the total N in the grain. Similarly, a recent study found that using NDVI combining the RE band at 730 nm and including textural information in different modeling methods gave the best results for estimating the total N in grain from booting to the early grain filling stage [72].

4.3. Spectral response of winter wheat varieties as related to grain yield, LAI, and straw yield

Traits that depend on dynamic morphological and physiological processes, such as grain yield, can be difficult to predict. To accurately estimate grain yield before harvest, morphological traits, such as plant height, ear density, above-ground biomass, and days to anthesis, as well as physiological traits, such as stomatal conductance and onset of senescence (stay green), have been used to account for the complex responses that determine grain yield [73,74]. Our findings show that straw and grain yield and LAI had strong relationships with VIs, particularly with those involving RE bands. The results also highlight the importance of the RE band centered at 705 nm. Moreover, the VIs NDRE717 (RE centered at 717 nm) and MCARI_740_MTVI (RE centered at 740 nm) showed the most consistent overall performance in predicting grain and straw yields, respectively. For LAI, there was no indication of one specific RE band, but VIs with several RE bands showed the best overall results (Fig. 4). At Changins, where both ground and aerial measurements could be done more intensively and consistently over the three years (2020, 2021, and 2022) of the study, there were strong relationships between VIs using different parts of the RE spectrum centered at 705, 717, and 740 nm and above-ground biomass at anthesis (data not shown), grain yield and straw yield (Fig. 4). Moreover, the close relationship between VIs using an RE band centered at 717 nm and LAI was of particular interest. The estimation of LAI by a ceptometer is a common practice by researchers that can be used as a proxy for biomass [75]. A UAV-based estimation of LAI is less time consuming than a ceptometer-based one, and as shown here, it can be achieved with an accuracy of $R^2 = 0.68$ (Fig. 6).

Besides providing good predictors of traits that are critical for wheat productivity, VIs with RE bands were also useful for predicting variables that are important for the sustainability of a farm operation, such as straw yield. Indeed, the variety CH_Nara, which is a very short variety in terms of plant height (Table 1), had low straw yield during the three years of trial (2020–2022) compared to the other varieties that were grown, namely CH Camedo (short), CH_Claro (short to intermediate), and Runal and Montalbano (intermediate). This wheat parameter seemed consistent over site and years, thus independent of environmental conditions, with lower straw yields, on average, for CH_Nara and CH_Camedo compared to other varieties. Straw yield was closely related to combined VIs, such as MCARI2_740_MTVI (RE band centered at 740 nm). This confirmed the relevance of using this VI to accurately estimate straw yield (Fig. 4) and to identify differences among varieties (Fig. 7). Clearly, it allowed for characterizing varieties with high (Montalbano, CH_Claro, and Runal) compared to low straw yields (CH_Nara and CH_Camedo).

Numerous studies have investigated wheat N response using multispectral or hyperspectral sensors, either ground-based [76,77], UAV-based [26,56,78–80], or through a combination of both approaches [81]. A hyperspectral sensor was used to estimate crop N from the tissue protein content [82]. However, the cost of hyperspectral sensors is prohibitive for most organizations carrying out N fertilization trials. Although UAV operation has become safer in recent years, other organizations are also reluctant to invest in hyperspectral sensors for UAVs, given the risk of a UAV crash or UAV flyaway.

Most studies using multispectral sensors combine VIs with a single RE band, typically centered around wavelengths such as 735 nm [26, 77], 730 nm [76], or 717 nm [56], to predict wheat traits, including canopy structure, biomass, N nutrition index, N uptake, plant N content, protein content, and grain yield. However, given the variability in wheat response analysis, it is important to consider biomass- and N status-related traits separately, as part of this variation is genotype-dependent. For instance, the variety CH_Nara is characterized by low biomass production and high canopy N content [65,66]. This example highlights the importance of specifically targeting different crop traits to accurately derive combined N-related components, such as

N uptake or NNI. Accordingly, this study emphasizes the advantage of using a multispectral sensor equipped with three RE bands to accurately characterize wheat variety responses linked to variety performance and sustainability across different environments. This observation was supported by the RF results, which highlighted the high importance of VIs with RE bands centered at 740 nm for predicting grain and straw yields. In contrast, VIs with RE centered at 705 nm were stronger predictors of total N content in biomass at anthesis. Notably, the most important feature was associated with the critical management period preceding the third N application, offering valuable insights for informed decision-making in winter wheat production. Recent studies have demonstrated the potential to improve NUE by adapting nitrogen application to specific field conditions [5,83,84], including small- to medium-scale fields typical of Swiss agriculture [26,85,86]. However, these approaches often rely on prescription maps derived from VIs calculated using only a single red-edge (RE) band. In the present study, we explored the potential of using RE band-specific VIs to enhance the accuracy of fertilization maps. This approach could support the development of more robust and transferable models for nitrogen management across diverse environments and multiple winter wheat varieties.

Nitrogen availability varies spatially and temporarily according to factors such as soil properties, management, and weather [87]. Besides the applications for N fertilization trials described here, UAVs allow for obtaining information from fields' spatial and temporal variability and, in turn, improve the utilization of fertilizer and reduce losses. Different field areas with similar N needs can be detected and treated accordingly by applying specific N fertilizer rates [88]. The N fertilizer application adapted to specific site conditions therefore allows for minimizing N leaching and greenhouse gas emissions [89]. Although satellites may show advantages in covering large fields, UAVs are particularly suitable for small and medium-size fields [26,85,86], as is mostly the case in Switzerland (Swiss Federal Statistical Office FSO) [45]. Moreover, UAVs are less affected by cloud cover, which can disturb data availability and quality from satellites. Additionally, important considerations in the use UAVs or satellites are the initial investment in UAVs and sensors, the time needed in UAV training and surveying, and data processing [90].

Follow-up studies to further develop these methods and deploy them should include a larger panel of winter wheat varieties and consider the impact of the differences in phenology on spectral responses. UAV-based indicators of biomass and grain production have shown promising potential to predict yield parameters in several other crops [55,91,92]. Furthermore, the findings of this study with supplemental RE bands could be evaluated in other important field crops as well as methods combining traits such as plant height and VIs [92,93] that use only a single VI [93,94] or multiple VIs [92,95,96]. New studies could further address additional spectral responses [96], combining VI predictions over time [96,97], and take advantage of developments in machine learning [58]. Although VIs incorporating the RE band centered at 705 nm showed a clearer and more consistent ability to predict N-related traits—such as chlorophyll content and total N in biomass at anthesis—this study did not deliver conclusive results about the potential of RE bands centered at 717 nm and 740 nm to predict grain yield, straw yield, and LAI. Relationship analyses indicated that VIs using the RE band at 717 nm were stronger predictors of grain yield, while those including the 740 nm RE band were more closely associated with straw yield. However, the RF analysis identified NDRE (with the RE band at 740 nm) as the most important feature for predicting both grain and straw yield. To further explore and better differentiate the predictive potential of these RE bands, future studies should consider using a broader panel of winter wheat varieties across a wider range of environments.

5. Conclusion

A 10-band multispectral sensor mounted on a UAV enabled the measurement of the biomass N content of winter wheat varieties grown in N fertilization trials located at different sites and across three seasons. This measurement is critical for providing NNI insights to farmers who manage N in winter wheat. Our findings suggest adding predictions of LAI, grain, and straw yield from multispectral UAV surveys to N fertilization trials, based on both the accuracy of these parameters and their potential superior cost-effectiveness compared to conventional approaches. As shown here, such integration can supplement the outcomes of N fertilization trials with useful information about NUE and residue management, a practice that affects soil carbon and fertility. We present evidence that including more RE bands in the evaluated sensor can allow for the estimation of VIs by combining specific RE bands to predict total N in aboveground biomass (RE band centered at 705 nm) and grain and straw yield (RE bands centered at 717 nm and at 740 nm). The VIs combining specific RE bands outperformed those proposed in previous studies using multispectral sensors. This spectral information can be used to support wheat N fertilization application, taking into account specific variety needs and environmental conditions.

Future research should incorporate a broader panel of varieties to better assess the accuracy of spectral data, accounting for variation in crop response due to phenological differences captured through time-series measurements. In addition, the experimental design should include fields cropped under conservation, organic, and regenerative agriculture to evaluate the stability and performance of vegetation indices under varying cropping systems. This will enhance the applicability of these indices across broader contexts. Building on this framework, future research should also expand to other crops, such as maize and barley and to diverse environmental stress scenarios such as drought that substantially influence response to N fertilization.

Developing automated UAVs data collection and processing pipelines with user-friendly platforms for smooth integration from flight planning to decision-making will maximize the use of UAVs and support real-time decisions. In addition, future research should be directed toward automating the integration of UAVs and satellite sensing plus weather information and artificial intelligence to develop a robust decision support system.

Data availability

Data will be made available on request. Source code and sample data for VI extraction and RF analysis are available on github (https://github.com/Nicodroneagro/VI-extraction-and-RF-analysis.git).

Funding

This work was supported by the Swiss Federal Office for Agriculture (project number 19.03), Agroscope, Swiss Granum, Schweizerischer Getreideproduzentenverband SGPV, Timac Agro, JOWA AG, Prometerre/Proconseil, Forum Ackerbau, and Groupe Culture Romandie. Juan M. Herrera was supported by the project INVITE from the Horizon 2020 Framework Programme of the European Union under Grant Agreement No 817,970 (https://www.h2020-invite.eu/).

CRediT authorship contribution statement

Nicolas Vuille-dit-Bille: Writing – review & editing, Writing – original draft, Methodology, Investigation, Formal analysis, Data curation. **Lilia Levy Häner:** Writing – review & editing, Supervision, Methodology, Funding acquisition, Conceptualization. **Silvan Strebel:** Writing – review & editing, Project administration, Investigation, Data curation. **Amanda Burton:** Writing – review & editing, Project administration, Methodology, Investigation, Data curation, Conceptualization. **Noémie Schaad:** Project administration, Methodology, Investigation, Data curation. **Didier Pellet:** Writing – review & editing, Supervision, Methodology, Funding acquisition, Conceptualization. **Nathalie Wuyts:** Writing – review & editing. **Simon Treier:** Writing – review & editing, Methodology. **Paola de F. Bongiovani:** Writing – review & editing,

Methodology. **Juan Manuel Herrera:** Writing – review & editing, Methodology, Funding acquisition, Formal analysis, Conceptualization.

Declaration of competing interest

The authors state that they have no conflicts of interest.

Acknowledgments

The authors would like to thank the Swiss Federal Office for Agriculture [project number 19.03], Agroscope, Swiss Granum, Schweizerischer Getreideproduzentenverband SGPV, Timac Agro, JOWA AG, Prometerre/Proconseil, Forum Ackerbau, and Groupe Culture Romandie for supporting and funding this project.

Supplementary materials

Supplementary material associated with this article can be found, in the online version, at doi:10.1016/j.atech.2025.101528.

References

[1] P.R. Ehrlich, J. Harte, To feed the world in 2050 will require a global revolution, Proc. Natl. Acad. Sci. 112 (2015) 14743–14744, https://doi.org/10.1073/pnas.1519841112.
[2] D.K. Ray, N.D. Mueller, P.C. West, J.A. Foley, Yield trends are insufficient to double global crop production by 2050, PLoS One 8 (2013) e66428, https://doi.org/10.1371/journal.pone.0066428.
[3] K.G. Cassman, A. Dobermann, Nitrogen and the future of agriculture: 20 years on, Ambio 51 (2022) 17–24, https://doi.org/10.1007/s13280-021-01526-w.
[4] F. Faostat, Agriculture organization corporate statistical database, Fertilizers (2022). http://www.fao.org/faostat/en/#data.
[5] B. Basso, C. Fiorentino, D. Cammarano, U. Schulthess, Variable rate nitrogen fertilizer response in wheat using remote sensing, Precis. Agric. 17 (2016) 168–182, https://doi.org/10.1007/s11119-015-9414-9.
[6] P. Jan, C. Calabrese, M. Lips, Determinants of nitrogen surplus at farm level in Swiss agriculture, Nutr. Cycl. Agroecosyst. 109 (2017) 133–148, https://doi.org/10.1007/s10705-017-9871-9.
[7] E. Spiess, Nitrogen, phosphorus and potassium balances and cycles of Swiss agriculture from 1975 to 2008, Nutr. Cycl. Agroecosyst. 91 (2011) 351–365, https://doi.org/10.1007/s10705-011-9466-9.
[8] L. Lassaletta, G. Billen, B. Grizzetti, J. Anglade, J. Garnier, 50 year trends in nitrogen use efficiency of world cropping systems: the relationship between yield and nitrogen input to cropland, Environ. Res. Lett. 9 (2014) 105011, https://doi.org/10.1088/1748-9326/9/10/105011.
[9] B.J. Zebarth, C.F. Drury, N. Tremblay, A.N. Cambouris, Opportunities for improved fertilizer nitrogen management in production of arable crops in eastern Canada: a review, Can. J. Soil Sci. 89 (2009) 113–132, https://doi.org/10.4141/CJSS07102.
[10] C. Zörb, U. Ludewig, M.J. Hawkesford, Perspective on wheat yield and quality with reduced nitrogen supply, Trends Plant Sci. 23 (2018) 1029–1037, https://doi.org/10.1016/j.tplants.2018.08.012.
[11] R. Flisch, R. Neuweiler, T. Kuster, H. Oberholzer, O. Huguenin-Elie, W. Richner, 2/ Caractéristiques et analyses du sol, in: W. Richner, S. Sinaj (Eds.), Principes De Fertilisation Des Cultures Agricoles En Suisse, Agrarforschung Schweiz, Agroscope, 2017. PRIF.
[12] T.F. Morris, T.S. Murrell, D.B. Beegle, J.J. Camberato, R.B. Ferguson, J. Grove, Q. Ketterings, P.M. Kyveryga, C.A.M. Laboski, J.M. McGrath, J.J. Meisinger, J. Melkonian, B.N. Moebius-Clune, E.D. Nafziger, D. Osmond, J.E. Sawyer, P. C. Scharf, W. Smith, J.T. Spargo, H.M. van Es, H. Yang, Strengths and limitations of nitrogen rate recommendations for corn and opportunities for improvement, Agron. J. 110 (2018) 1–37, https://doi.org/10.2134/agronj2017.02.0112.
[13] F.E. Miguez, H. Poffenbarger, How can we estimate optimum fertilizer rates with accuracy and precision? Agric. Environ. Lett. 7 (2022) e20075 https://doi.org/10.1002/ael2.20075.
[14] L.L. Häner, C. Brabant, L'art de fractionner l'azote pour optimiser le rendement et la teneur en protéines du blé, Rech. Agron. Suisse. 7 (2016) 80–87.
[15] A. Burton, L.L. Häner, N. Schaad, S. Strebel, N. Vuille-dit-Bille, P.D.F. Bongiovani, A. Holzkämper, D. Pellet, J.M. Herrera, Evaluating nitrogen fertilization strategies to optimize yield and grain nitrogen content in top winter wheat varieties across Switzerland, Field Crops Res. 307 (2024) 109251, https://doi.org/10.1016/j.fcr.2024.109251.
[16] Z. Khan, J. Chopin, J. Cai, V.-R. Eichi, S. Haefele, S. Miklavcic, Quantitative estimation of wheat phenotyping traits using ground and aerial imagery, Remote Sens. 10 (2018) 950, https://doi.org/10.3390/rs10060950.
[17] S. Nawar, R. Corstanje, G. Halcro, D. Mulla, A.M. Mouazen, Delineation of soil management zones for variable-rate fertilization, Adv. Agron. 143 (2017) 175–245, https://doi.org/10.1016/bs.agron.2017.01.003. Elsevier.
[18] J.U.H. Eitel, D.S. Long, P.E. Gessler, A.M.S. Smith, Using in-situ measurements to evaluate the new RapidEye TM satellite series for prediction of wheat nitrogen status, Int. J. Remote Sens. 28 (2007) 4183–4190, https://doi.org/10.1080/01431160701422213.
[19] A.A. Gitelson, Y.J. Kaufman, M.N. Merzlyak, Use of a green channel in remote sensing of global vegetation from EOS-MODIS, Remote Sens. Environ. 58 (1996) 289–298.
[20] A. Matese, P. Toscano, S. Di Gennaro, L. Genesio, F. Vaccari, J. Primicerio, C. Belli, A. Zaldei, R. Bianconi, B. Gioli, Intercomparison of UAV, aircraft, and satellite remote sensing platforms for precision viticulture, Remote Sens. 7 (2015) 2971–2990, https://doi.org/10.3390/rs70302971.
[21] A. Walter, R. Khanna, P. Lottes, C. Stachniss, J. Nieto, F. Liebisch, Flourish—a robotic approach for automation in crop management, Proc. Int. Conf. Precis. Agric. (ICPA) (2018).
[22] J.-B. Féret, K. Berger, F. De Boissieu, Z. Malenovský, PROSPECT-PRO for estimating content of nitrogen-containing leaf proteins and other carbon-based constituents, Remote Sens. Environ. 252 (2021) 112173, https://doi.org/10.1016/j.rse.2020.112173.
[23] F. Liebisch, G. Kung, A. Damm, A. Walter, Characterization of crop vitality and resource use efficiency by means of combining imaging spectroscopy based plant traits, 2014 6th Workshop on Hyperspectral image and signal processing, Evol. Remote Sens. (2014) 1–4, https://doi.org/10.1109/WHISPERS.2014.8077612.
[24] L. Prey, U. Schmidhalter, Sensitivity of vegetation indices for estimating vegetative status in winter wheat, Sensors 19 (2019) 3712, https://doi.org/10.3390/s19173712.
[25] J. González-Piqueras, H. Lopez-Corcoles, S. Sánchez, J. Villodre, V. Bodas, I. Campos, A. Osann, A. Calera, Monitoring crop N status by using red edge-based indices, Adv. Anim. Biosci. 8 (2017) 338–342, https://doi.org/10.1016/j.fcr.2013.12.018.
[26] F. Argento, T. Anken, F. Abt, E. Vogelsanger, A. Walter, F. Liebisch, Site-specific nitrogen management in winter wheat supported by low-altitude remote sensing and soil data, Precis. Agric. 22 (2021) 364–386, https://doi.org/10.1007/s11119-020-09733-3.
[27] G.M. Bean, N.R. Kitchen, J.J. Camberato, R.B. Ferguson, F.G. Fernandez, D. W. Franzen, C.A.M. Laboski, E.D. Nafziger, J.E. Sawyer, P.C. Scharf, J. Schepers, J. S. Shanahan, Active-optical reflectance sensing corn algorithms evaluated over the United States Midwest corn belt, Agron. J. 110 (2018) 2552–2565, https://doi.org/10.2134/agronj2018.03.0217.
[28] H. Li, Y. Zhang, Y. Lei, V. Antoniuk, C. Hu, Evaluating different non-destructive estimation methods for winter wheat (Triticum aestivum L.) nitrogen status based on canopy spectrum, Remote Sens. 12 (2019) 95.
[29] D. Rodriguez, G.J. Fitzgerald, R. Belford, L.K. Christensen, Detection of nitrogen deficiency in wheat from spectral reflectance indices and basic crop eco-physiological concepts, Aust. J. Agric. Res. 57 (2006) 781, https://doi.org/10.1071/AR05361.
[30] G.J. Fitzgerald, D. Rodriguez, L.K. Christensen, R. Belford, V.O. Sadras, T.R. Clarke, Spectral and thermal sensing for nitrogen and water status in rainfed and irrigated wheat environments, Precis. Agric. 7 (2006) 233–248, https://doi.org/10.1007/s11119-006-9011-z.
[31] D. Cammarano, G. Fitzgerald, R. Casa, B. Basso, Assessing the robustness of vegetation indices to estimate wheat N in Mediterranean environments, Remote Sens. 6 (2014) 2827–2844, https://doi.org/10.3390/rs6042827.
[32] International Soil Reference and Information Centre, SoilGrids. (https://www.isric.org/explore/soilgrids) Determination of a critical nitrogen dilution curve for winter wheat crops, Ann. Bot. 74 (2020) 10.
[33] Swiss Granum, Recommended list, https://www.swissgranum.ch/fileadmin/user_upload/swiss-granum/dokumente/Richtlinien/Sortenlisten/2025/LR2025_Ble_aut_F.pdf, 2021. Accessed 7 May 2024.
[34] C.I. Fernández, B. Leblon, A. Haddadi, K. Wang, J. Wang, Potato late blight detection at the leaf and canopy levels based in the red and red-edge spectral regions, Remote Sens. 12 (2020) 1292, https://doi.org/10.3390/rs12081292.
[35] D. Haboudane, J.R. Miller, E. Pattey, P.J. Zarco-Tejada, I.B. Strachan, Hyperspectral vegetation indices and novel algorithms for predicting green LAI of crop canopies: modeling and validation in the context of precision agriculture, Remote Sens. Environ. 90 (2004) 337–352, https://doi.org/10.1016/j.rse.2003.12.013.
[36] J.M. Chen, Evaluation of vegetation indices and a modified simple ratio for boreal applications, Can. J. Remote Sens. 22 (1996) 229–242, https://doi.org/10.1080/07038992.1996.10855178.
[37] D.A. Sims, J.A. Gamon, Relationships between leaf pigment content and spectral reflectance across a wide range of species, leaf structures and developmental stages, Remote Sens. Environ. 81 (2002) 337–354, https://doi.org/10.1016/S0034-4257(02)00010-X.
[38] R, Analysing nitrogen responses of cereals to prioritize routes to the improvement of nitrogen use efficiency, J. Exp. Bot. 60 (2009) 1939–1951, https://doi.org/10.1093/jxb/erp116.
[39] F.I. Matias, M.V. Caraza-Harter, J.B. Endelman, FIELDimageR: an R package to analyze orthomosaic images from agricultural field trials, Plant Phenome. J. 3 (1) e20005. https://doi.org/10.1002/ppj2.20005.
[40] S. Sankaran, L.R. Khot, A.H. Carter, Field-based crop phenotyping: multispectral aerial imaging for evaluation of winter wheat emergence and spring stand, Comput. Electron. Agric. 118 (2015) 372–379, https://doi.org/10.1016/j.compag.2015.09.001.
[41] L. Breiman, Random forests, Mach. Learn. 45 (2001) 5–32.
[42] A.M. Lapaz Olveira, M. Castro-Franco, H.R. Saínz Rozas, et al., Monitoring corn nitrogen nutrition index from optical and synthetic aperture radar satellite data and soil available nitrogen, Precis. Agric. 24 (2023) 2592–2606, https://doi.org/10.1007/s11119-023-10054-4.

[43] J. Huang, et al., Assimilation of remote sensing into crop growth models: current status and perspectives, Agric. Meteorol. 276 (2019) 107609.
[44] Y. Zhao, A.B. Potgieter, M. Zhang, B. Wu, G.L. Hammer, Predicting wheat yield at the field scale by combining high-resolution Sentinel-2 satellite imagery and crop modelling, Remote Sens. 12 (2020) 1024, https://doi.org/10.3390/rs12061024.
[45] FSO, Agriculture and food: pocket statistics 2024. Swiss Federal Statistical Office. Retrieved November 22, 2024, from https://www.bfs.admin.ch/bfs/en/home/statistics/agriculture-forestry/farming.assetdetail.8706379.html.
[46] B. Hansen, L. Thorling, J. Schullehner, M. Termansen, T. Dalgaard, Groundwater nitrate response to sustainable nitrogen management, Sci. Rep. 7 (2017) 8566, https://doi.org/10.1038/s41598-017-07147-2.
[47] K.A. Congreves, et al., Nitrogen use efficiency definitions of today and tomorrow, Front. Plant Sci. 12 (2021) 637108.
[48] R. Sylvester-Bradley, D.R. Kindred, Analysing nitrogen responses of cereals to prioritize routes to the improvement of nitrogen use efficiency, J. Exp. Bot. 60 (2009) 1939–1951, https://doi.org/10.1093/jxb/erp116.
[49] F. Cormier, S. Faure, P. Dubreuil, E. Heumez, K. Beauchêne, S. Lafarge, S. Praud, J. Gouis, A multi-environmental study of recent breeding progress on nitrogen use efficiency in wheat (Triticum aestivum L.), Theor. Appl. Genet. 126 (2013) 3035–3048, https://doi.org/10.1007/s00122-013-2191-9.
[50] M. Bogard, V. Allard, M. Brancourt-Hulmel, E. Heumez, J.-M. Machet, M.-H. Jeuffroy, P. Gate, P. Martre, J. Gouis, Deviation from the grain protein concentration–grain yield negative relationship is highly correlated to post-anthesis N uptake in winter wheat, J. Exp. Bot. 61 (2010) 4303–4312, https://doi.org/10.1093/jxb/erq238.
[51] European Commission, Proposal for a regulation of the European Parliament and of the Council on the production and marketing of plant reproductive material in the Union (2023).
[52] H. Blanco-Canqui, R. Lal, Crop residue removal impacts on soil productivity and environmental quality, CRC Crit. Rev. Plant Sci. 28 (2009) 139–163, https://doi.org/10.1080/07352680902776507.
[53] J. Dai, B. Bean, B. Brown, W. Bruening, J. Edwards, M. Flowers, R. Karow, C. Lee, G. Morgan, M. Ottman, Harvest index and straw yield of five classes of wheat, Biomass Bioenergy 85 (2016) 223–227, https://doi.org/10.1016/j.biombioe.2015.12.023.
[54] C. Wang, W. Liu, Q. Li, D. Ma, H. Lu, W. Feng, Y. Xie, Y. Zhu, T. Guo, Effects of different irrigation and nitrogen regimes on root growth and its correlation with above-ground plant parts in high-yielding wheat under field conditions, Field Crops Res. 165 (2014) 138–149, https://doi.org/10.1016/j.fcr.2014.04.011.
[55] U.S. Panday, N. Shrestha, S. Maharjan, A.K. Pratihast, Shahnawaz, K.L. Shrestha, J. Aryal, Correlating the plant height of wheat with above-ground biomass and crop yield using drone imagery and crop surface model: a case study from Nepal, Drones 4 (2020) 28.
[56] O.S. Walsh, J.M. Marshall, E. Nambi, C.A. Jackson, E.O. Ansah, R. Lamichhane, J. McClintick-Chess, F. Bautista, Wheat yield and protein estimation with handheld and unmanned aerial vehicle-mounted sensors, Agronomy 13 (2023) 207, https://doi.org/10.3390/agronomy13010207.
[57] W.A. Smith, L.M. Wendt, I.J. Bonner, J.A. Murphy, Effects of storage moisture content on corn stover biomass stability, composition, and conversion efficacy, Front. Bioeng. Biotechnol. 8 (2020) 716, https://doi.org/10.3389/fbioe.2020.00716.
[58] J. Wang, S. Meyer, X. Xu, W.W. Weisser, K. Yu, Drone multispectral imaging captures the effects of soil nmin on canopy structure and nitrogen use efficiency in wheat, Available at SSRN 4699313 (2024).
[59] M.L. Stone, J.B. Solie, W.R. Raun, R.W. Whitney, S.L. Taylor, J.D. Ringer, Use of spectral radiance for correcting in-season fertilizer nitrogen deficiencies in winter wheat, Trans. ASAE 39 (1996) 1623–1631, https://doi.org/10.13031/2013.27678.
[60] D. Zhao, K.R. Reddy, V.G. Kakani, V.R. Reddy, Nitrogen deficiency effects on plant growth, leaf photosynthesis, and hyperspectral reflectance properties of sorghum, Eur. J. Agron. 22 (2005) 391–403, https://doi.org/10.1016/j.eja.2004.06.005.
[61] L. Sharma, S. Bali, A review of methods to improve nitrogen use efficiency in agriculture, Sustainability 10 (2017) 51, https://doi.org/10.3390/su10010051.
[62] Y. Gu, B.K. Wylie, D.M. Howard, K.P. Phuyal, L. Ji, NDVI saturation adjustment: a new approach for improving cropland performance estimates in the Greater Platte River Basin, USA, Ecol. Indic. 30 (2013) 1–6.
[63] A. Jensen, B. Lorenzen, H.S. Østergaard, E.K. Hvelplund, Radiometric estimation of biomass and nitrogen content of barley grown at different nitrogen levels, Int. J. Remote Sens. 11 (1990) 1809–1820, https://doi.org/10.1080/01431169008955131.
[64] H. Van Keulen, J. Goudriaan, N. Seligman, Modelling the effects of nitrogen on canopy development and crop growth, in: Plant Canopies: Their Growth, Form and Function (1989) 83–104.
[65] C. Caldelas, F.Z. Rezzouk, N.A. Gutiérrez, M.C. Diez–Fraile, J.L.A. Ortega, Interaction of genotype, water availability, and nitrogen fertilization on the mineral content of wheat grain, Food Chem. 404 (2023) 134565, https://doi.org/10.1016/j.foodchem.2022.134565.
[66] P.D.F. Bongiovani, E. Frossard, R. De S. Nóia Júnior, S. Asseng, N. Vuille-dit-Bille, A. Burton, J.M. Herrera, Responses of winter wheat genotypes to reduced rainfall, nitrogen fertilization and pre-crops in Switzerland, Field Crops Res. 308 (2024) 109272, https://doi.org/10.1016/j.fcr.2024.109272.
[67] J.U.H. Eitel, D.S. Long, P.E. Gessler, E.R. Hunt, Combined spectral index to improve ground-based estimates of nitrogen status in dryland wheat, Agron. J. 100 (2008) 1694–1702, https://doi.org/10.2134/agronj2007.0362.
[68] J. Dash, P.J. Curran, Evaluation of the MERIS terrestrial chlorophyll index (MTCI), Adv. Space Res. 39 (2017) 100–104, https://doi.org/10.1016/j.asr.2006.02.034.
[69] F.M. Padilla, R. De Souza, M.T. Peña-Fleitas, M. Gallardo, C. Giménez, R. B. Thompson, Different responses of various chlorophyll meters to increasing nitrogen supply in sweet pepper, Front. Plant Sci. 9 (2018) 1752, https://doi.org/10.3389/fpls.2018.01752.
[70] S. Christensen, J. Goudriaan, Deriving light interception and biomass from spectral reflectance ratio, Remote Sens. Environ. 43 (1993) 87–95, https://doi.org/10.1016/0034-4257(93)90066-7.
[71] A.A. Gitelson, Y. Gritz, M.N. Merzlyak, Relationships between leaf chlorophyll content and spectral reflectance and algorithms for non-destructive chlorophyll assessment in higher plant leaves, J. Plant Physiol. 160 (2003) 271–282, https://doi.org/10.1078/0176-1617-00887.
[72] Z. Fu, Combining UAV multispectral imagery and ecological factors to estimate leaf nitrogen and grain protein content of wheat, Eur. J. Agron. (2022).
[73] M. Faralli, Exploiting natural variation and genetic manipulation of stomatal conductance for crop improvement, Curr. Opin. Plant Biol. (2019).
[74] N.M. Kamal, Y.S.A. Gorafi, M. Abdelrahman, E. Abdellatef, H. Tsujimoto, Stay-green trait: a prospective approach for yield potential, and drought and heat stress adaptation in globally important cereals, Int. J. Mol. Sci. 20 (2019) 5837.
[75] B.R. Pandey, W.A. Burton, P.A. Salisbury, M.E. Nicolas, Non-destructive measurement of canopy cover is an alternative to biomass sampling at anthesis to predict the yield of canola-quality 'Brassica juncea, Aust. J. Crop Sci. 10 (2016) 482–489.
[76] H. Li, D. Li, K. Xu, W. Cao, X. Jiang, J. Ni, Monitoring of nitrogen indices in wheat leaves based on the integration of spectral and canopy structure information, Agronomy 12 (2022) 833.
[77] W. Wang, X. Yao, X. Yao, Y. Tian, X. Liu, J. Ni, W. Cao, Y. Zhu, Estimating leaf nitrogen concentration with three-band vegetation indices in rice and wheat, Field Crops Res. 129 (2012) 90–98.
[78] M. Shu, Z. Wang, W. Guo, H. Qiao, Y. Fu, Y. Guo, L. Wang, Y. Ma, X. Gu, Effects of variety and growth stage on UAV multispectral estimation of plant nitrogen content of winter wheat, Agriculture 14 (2024) 1775, https://doi.org/10.3390/agriculture14101775.
[79] G. Astaoui, J.E. Dadaiss, I. Sebari, S. Benmansour, E. Mohamed, Mapping wheat dry matter and nitrogen content dynamics and estimation of wheat yield using UAV multispectral imagery machine learning and a variety-based approach: case study of Morocco, AgriEngineering 3 (2021) 29–49, https://doi.org/10.3390/agriengineering3010003.
[80] R.N. Sahoo, R. Rejith, S. Gakhar, R. Ranjan, M.C. Meena, A. Dey, J. Mukherjee, R. Dhakar, A. Meena, A. Daas, Drone remote sensing of wheat N using hyperspectral sensor and machine learning, Precis. Agric. 25 (2024) 704–728.
[81] X. Song, G. Yang, X. Xu, D. Zhang, C. Yang, H. Feng, Winter wheat nitrogen estimation based on ground-level and UAV-mounted sensors, Sensors 22 (2022) 549.
[82] K. Berger, J. Verrelst, J.-B. Féret, Z. Wang, M. Wocher, M. Strathmann, M. Danner, W. Mauser, T. Hank, Crop nitrogen monitoring: recent progress and principal developments in the context of imaging spectroscopy missions, Remote Sens. Environ. 242 (2020) 111758, https://doi.org/10.1016/j.rse.2020.111758.
[83] J. Cohan, B. Soenen, G. Vericel, F. Laurent, Improving nitrogen use efficiency in wheat: recent progress and prospects in France, proceedings of Phloème, First Biennials of Cereal Innovation, Paris, 24th–25th January (2018).
[84] W.R. Raun, J.B. Solie, G.V. Johnson, M.L. Stone, R.W. Mullen, K.W. Freeman, W. E. Thomason, E.V. Lukina, Improving nitrogen use efficiency in cereal grain production with optical sensing and variable rate application, Agron. J. 94 (2002) 815–820.
[85] J. Van Loon, A. Speratti, L. Gabarra, B. Govaerts, Precision for smallholder farmers: a small-scale-tailored variable rate fertilizer application kit, Agriculture 8 (2018) 48, https://doi.org/10.3390/agriculture8040048.
[86] X. Wang, Y. Miao, R. Dong, Y. Guan, D. Mulla, Evaluating the Potential Benefits of Field-Specific Nitrogen Management of Spring Maize in Northeast China, Precision Agriculture, Wageningen Academic Publishers, 2019, p. 469.
[87] D.R. Kindred, A.E. Milne, R. Webster, B.P. Marchant, R. Sylvester-Bradley, Exploring the spatial variation in the fertilizer-nitrogen requirement of wheat within fields, J Agric. Sci. 153 (2015) 25–41, https://doi.org/10.1017/S0021859613000919.
[88] B. Basso, D. Cammarano, C. Fiorentino, J.T. Ritchie, Wheat yield response to spatially variable nitrogen fertilizer in mediterranean environment, Eur. J. Agron. 51 (2013) 65–70, https://doi.org/10.1016/j.eja.2013.06.007.
[89] A. Walter, R. Finger, R. Huber, N. Buchmann, Smart farming is key to developing sustainable agriculture, Proc. Natl. Acad. Sci. 114 (2017) 6148–6150, https://doi.org/10.1073/pnas.1707462114.
[90] E.R. Hunt, C.S.T. Daughtry, What good are unmanned aircraft systems for agricultural remote sensing and precision agriculture? Int. J. Remote Sens. 39 (2018) 5345–5376, https://doi.org/10.1080/01431161.2017.1410300.
[91] M.G. Acorsi, F. Das Dores Abati Miranda, M. Martello, D.A. Smaniotto, L.R. Sartor, Estimating biomass of black throat using UAV-based RGB imaging, Agronomy 9 (2019) 344, https://doi.org/10.3390/agronomy9070344.
[92] N. Tilly, D. Hoffmeister, Q. Cao, V. Lenz-Wiedemann, Y. Miao, G. Bareth, Transferability of models for estimating paddy rice biomass from spatial plant height data, Agriculture 5 (2015) 538–560, https://doi.org/10.3390/agriculture5030538.
[93] S. Guan, K. Fukami, H. Matsunaka, M. Okami, R. Tanaka, H. Nakano, T. Sakai, K. Nakano, H. Ohdan, K. Takahashi, Assessing correlation of high-resolution NDVI with fertilizer application level and yield of rice and wheat crops using small UAVs, Remote Sens. 11 (2019) 112.

[94] K.C. Swain, S.J. Thomson, P.W. Jayasuriya, Adoption of an unmanned helicopter for low-altitude remote sensing to estimate yield and total biomass of a rice crop, Trans. ASABE 53 (2010) 21–27, https://doi.org/10.13031/2013.29493.
[95] D. Fawcett, C. Panigada, G. Tagliabue, M. Boschetti, M. Celesti, A. Evdokimov, K. Biriukova, R. Colombo, F. Miglietta, U. Rascher, Multi-scale evaluation of drone-based multispectral surface reflectance and vegetation indices in operational conditions, Remote Sens. 12 (2020) 514.
[96] X. Zhou, H.B. Zheng, X.Q. Xu, J.Y. He, X.K. Ge, X. Yao, T. Cheng, Y. Zhu, W.X. Cao, Y.C. Tian, Predicting grain yield in rice using multi-temporal vegetation indices from UAV-based multispectral and digital imagery, ISPRS J. Photogramm. Remote Sens. 130 (2017) 246–255, https://doi.org/10.1016/j.isprsjprs.2017.05.003.
[97] R. Näsi, N. Viljanen, J. Kaivosoja, K. Alhonoja, T. Hakala, L. Markelin, E. Honkavaara, Estimating biomass and nitrogen amount of barley and grass using UAV and aircraft based spectral and photogrammetric 3D features, Remote Sens. 10 (2018) 1082, https://doi.org/10.3390/rs10071082.